AD-770 092

PROJECT CHASER: PHOTOMETER SENSOR PACKAGE

Frederick F. Marmo

GCA Corporation

Prepared for:

Air Force Office of Scientific Research

January 1973

DISTRIBUTED BY:

NTIS

National Technical Information Service
U. S. DEPARTMENT OF COMMERCE
5285 Port Royal Road, Springfield Va. 22151

Security Classification

DOCUMENT CONTROL DATA - R & D AD 770 092

(Security classification of title, body of abstract and indexing annotation must be entered when the overall report is classified)

1. ORIGINATING ACTIVITY (Corporate author)
GCA CORPORATION
GCA TECHNOLOGY DIVISION
BEDFORD, MASSACHUSETTS 01730

2a. REPORT SECURITY CLASSIFICATION
UNCLASSIFIED

2b. GROUP
N/A

3. REPORT TITLE
PROJECT CHASER

4. DESCRIPTIVE NOTES (Type of report and inclusive dates)
Scientific. Final. 15 June 1970 - 31 December 1972
Approved 17 July 1973

5. AUTHOR(S) (First name, middle initial, last name)

6. REPORT DATE	7a. TOTAL NO. OF PAGES	7b. NO. OF REFS
January 1973	96	0

8a. CONTRACT OR GRANT NO.
F19629-70-C-0294

b. PROJECT NO.
8627-01-02

c. DOD ELEMENT 61102F

d. DOD SUBELEMENT 681310

9a. ORIGINATOR'S REPORT NUMBER(S)
GCA-TR-73-1-A

9b. OTHER REPORT NO(S) (Any other numbers that may be assigned this report)
AFCRL TR-73-0338

10. DISTRIBUTION STATEMENT
A - Approved for public release; distribution unlimited.

11. SUPPLEMENTARY NOTES
TECH, Other

12. SPONSORING MILITARY ACTIVITY
Air Force Cambridge Research (Laboratories (LK)
L.G. Hanscom Field
Bedford, Massachusetts 01730

13. ABSTRACT

Rocketborne photometers were designed, tested, installed, and successfully flown in a series of field operations as part of Project CHASER, for observing missile exhaust plumes in a restricted spectral region. The equipment consisted of several alternative daytime/nighttime and photometric/imaging modes. A special baffling system was incorporated which provided high off-axis rejection of stray light for daytime baffling system. Additionally, a mechanical belt scanner was employed to derive target imaging information.

This report includes discussions of the instrumentation employed as well as those source and background factors which affect the design and field operation of the system.

DD FORM 1 NOV 65 1473 REPLACES DD FORM 1473, 1 JAN 64, WHICH IS OBSOLETE FOR ARMY USE.

UNCLASSIFIED
Security Classification

92

UNCLASSIFIED

Security Classification

14. KEY WORDS	LINK A ROLE	LINK A WT	LINK B ROLE	LINK B WT	LINK C ROLE	LINK C WT
Surveillance Vacuum Ultraviolet Photometer Rocket Instrumentation (Allow AFCRL to delete or add as desired)						

UNCLASSIFIED

Security Classification

AFCRL-TR-73-0338 GCA-TR-73-1-A

PROJECT CHASER: PHOTOMETER SENSOR PACKAGE

by

Frederick F. Marmo

GCA CORPORATION
GCA TECHNOLOGY DIVISION
Bedford, Massachusetts 01730

Contract No. F19628-70-C-0294
Project No. 8627
Task No. 862701
Work Unit No. 86270102

FINAL REPORT

January 1973

Contract Monitor: Robert E. Huffman
Aeronomy Laboratory

Approved for public release; distribution unlimited

Prepared for

AIR FORCE CAMBRIDGE RESEARCH LABORATORIES
AIR FORCE SYSTEMS COMMAND
UNITED STATES AIR FORCE
BEDFORD, MASSACHUSETTS 01730

ic

Qualified requestors may obtain additional copies from the Defense Documentation Center. All others should apply to the National Technical Information Service.

ABSTRACT

Rocketborne photometers were designed, tested, installed, and successfully flown in a series of field operations as part of Project CHASER, for observing missile exhaust plumes in a restricted spectral region. The equipment consisted of several alternative daytime/nighttime and photometric/imaging modes. A special baffling system was incorporated which provided high off-axis rejection of stray light for daytime baffling system. Additionally, a mechanical belt scanner was employed to derive target imaging information.

This report includes discussions of the instrumentation employed as well as those source and background factors which affect the design and field operation of the system.

PREVIOUS CONTRACTS

GCA has been involved in the general technical areas addressed in the present report as evidenced by the following list of previously conducted contracts:

Inclusive Dates	Agency	Contract No.	Contract Title
5 May 1969 - 1 February 1970	Lockheed (Prime to SAMSO)	B25-09770	VUV Surveillance
1 March 1968 - 1 February 1969	ASD	F33615-68-C-1463	UV Detection
1 June 1966 - 30 August 1967	ASD	AF33(615)-5075	VUV Surveillance
15 April 1965 - 14 June 1966	ASD	AF33(615)-2802	VUV Surveillance Techniques
3 April 1964 - 20 April 1965	ASD	AF33(615)-1675	VUV Surveillance Techniques
15 June 1962 - 30 July 1963	ASD	AF33(657)-9199	Surveillance Techniques in VUV

The following scientists and engineers have been actively engaged in the contract work reported herein:

C. Accardo
H. deWeerd
J. Dulchinos
A. Engelman
J. Horan
L. Johnson
F. Marmo
H. Miranda
P. Nordberg
C. Pike
F. Wanko

Table of Contents

List of Tables and Figures

List of Figures (continued)

I. MULTICHANNEL ROCKET-BORNE PHOTOMETER SYSTEM

The initial phase of this program involved the development of the standard multichannel rocket-borne photometer system. Each photometer of this system was built with a provision for the attachment of any combination of three optional accessory items in order to conform to the philosophy of design flexibility established during the initial design review phases of the program. The optional accessory items are a fixed filter assembly, a reticle scanning assembly, and an in-out (flip) filter assembly.

Three photometer instruments were designed to respond to signals in specific wavelength bands. Three additional instruments, identical to the three for the system were provided as operational spares. Photometer #1 represents the design option with an in-out filter attachment, photometer #2 represents the design option which makes use of the reticle motor attachment, and photometer #3 represents the design option with the fixed filter accessory. The six photometer instruments were intially designed for nighttime use so that maximum throughput was achieved by providing a nominal degree of baffling. However, each of the photometer instruments were later converted to the daytime version wherein much more baffling was required; sufficient baffling was achieved but with a loss of 60 to 70 percent of the original nighttime sensitivity. An additional modification involved the employment of a belt scanning device in the focal plane to acquire information on target spatial features.

The optical mechanical and electrical design details of the CHASER photometer systems are discussed in detail in the following two sections. Section II deals primarily in mechanical and optical aspects of the basic initial nighttime photometer design. Mechanical assembly procedures and methods of achieving optical alignment are also discussed in this section.

The electronics portion of the photometer system is described in detail in Section III which includes block diagram and circuit diagram

descriptions and a discussion of the theory of operation of the various circuit elements in the system.

Sections IV and V deal with the design, fabrication, test and calibration tasks associated with the daytime modification (baffle plate systems) and belt scanning systems, respectively. Where the indicated modifications involved corresponding changes in the mechanical, electronic circuitry and/or mode of operation, then these factors have also been identified and discussed in sufficient detail.

II. MECHANICAL AND OPTICAL DESIGN

A. INTRODUCTION

Each photometer consists of a basic telescope and a number of attachments; a drawing of the complete assembly is shown in Figure 1. The telescope consists of a primary mirror and a sensor which is installed in the primary focal plane. The attachments consist of the following: a rotating reticle, a fixed optical filter and an optical filter which can be moved into and out of the focal plane. The attachments can be installed on the basic telescope in any combination. Each of these entities is discussed below.

B. INSTALLATION, ALIGNMENT AND DESIGN DETAILS OF BASIC SYSTEM

1. The Basic Telescope

The components that constitute the basic instrument are shown in Figure 2 for the nighttime version. The telescope structure is a dipbrazed assembly consisting of two concentric tubes with the inner tube rigidly supported by two 3 spoke spiders (see Figure 3). The inner tube provides a mounting interface for the sensor (a photomultiplier tube in all cases) and the outer tube presents a mounting interface for the optical filter and the rotating reticle.

The outer tube is attached to the payload structure via the front plate (shown installed in Figure 3) and via the base plate of the mirror assembly.

2. Aligning the Optical Axis

In order to simplify the optical alignment checks in a fully integrated system, each photometer is provided with an alignment mirror which defines the pointing direction of the instrument. Each instrument prior to shipment is aligned such that the optical axis of the primary mirror is parallel to the normal of the alignment mirror. The alignment mirror is located underneath the left cap, as shown in Figures 1 and 2, and is permanently attached to three pads, which are machined on the top surface of the front plate. This done to ensure

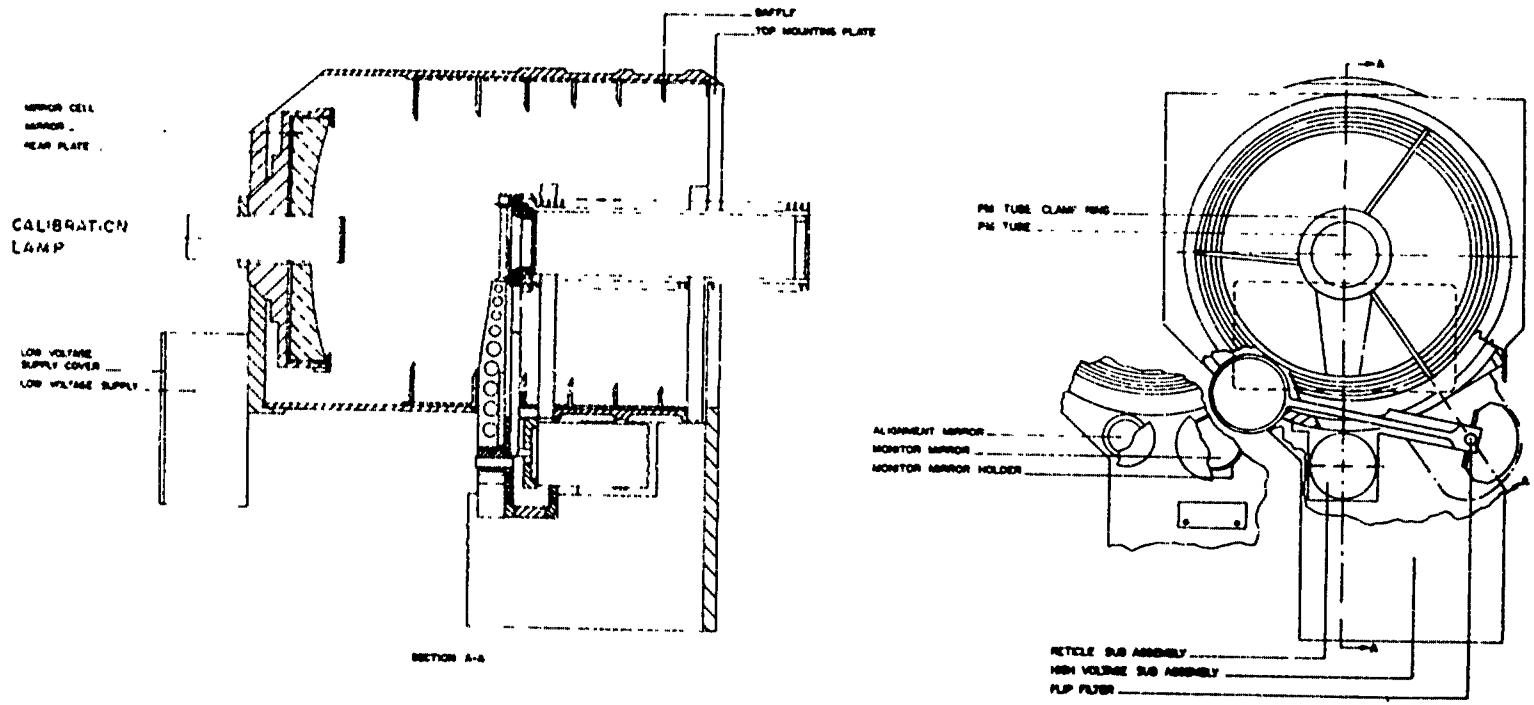

Figure 1. CHASER Photometer M4

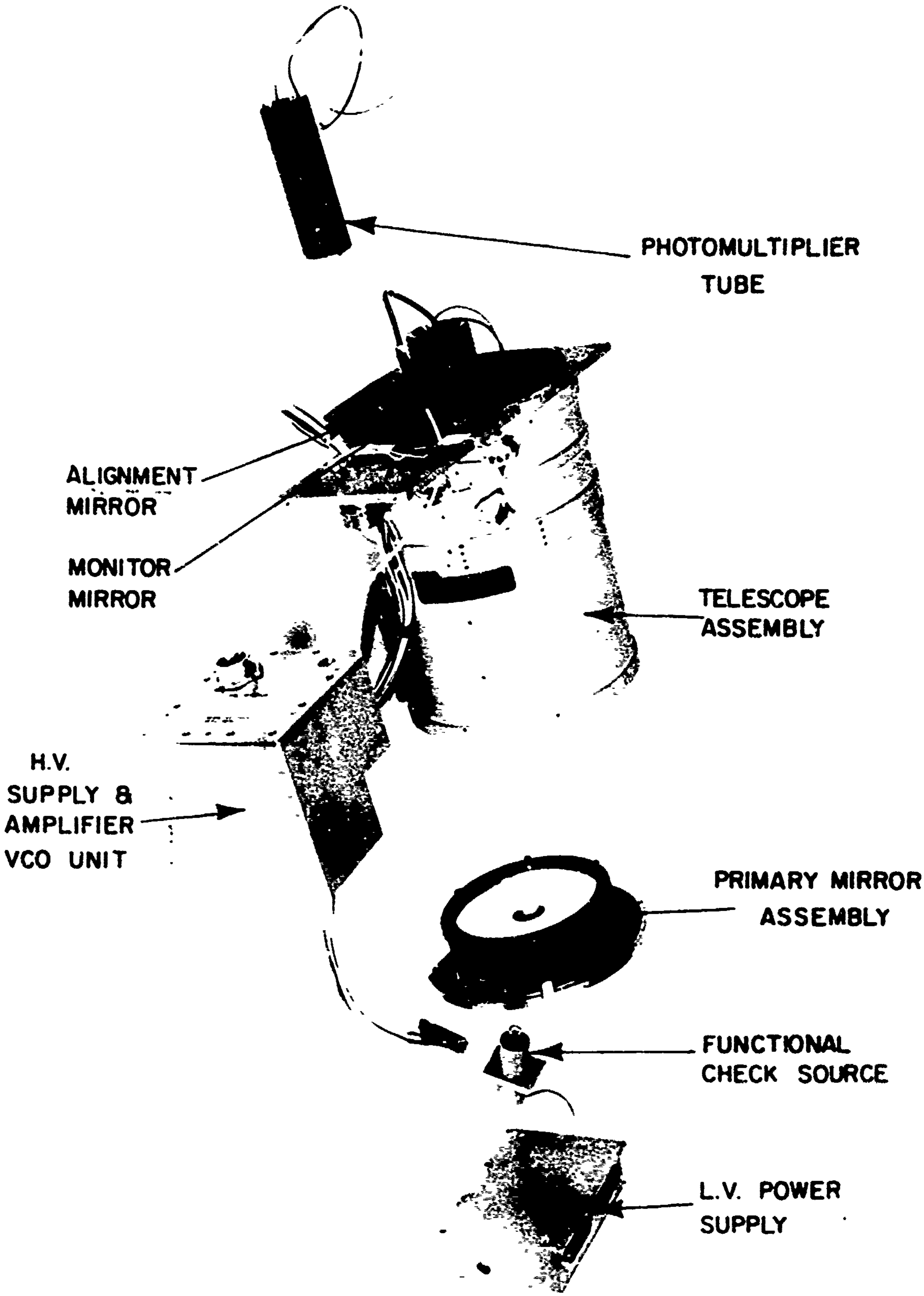

Figure 2. Exploded view of GCA photometer.

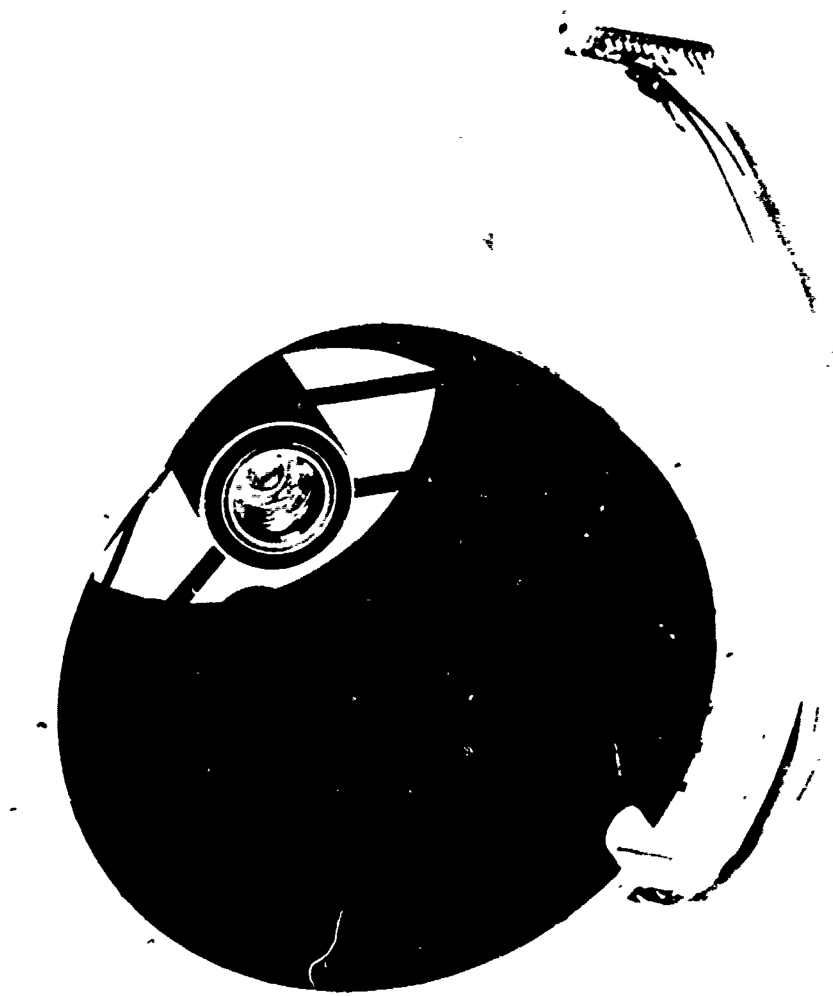

Figure 3. Telescope housing with PM tube installed.

that the plane of the alignment mirror is parallel to the front plate whose normal is used as the optical reference when interfacing with other systems.

The primary mirror is aligned to the alignment mirror as follows: a laser or auto collimator is used to bore sight the alignment mirror and primary mirror sequentially and the primary mirror is adjusted until a satisfactory alignment is obtained. The instrument is rigidly installed with the optical axis in a horizontal plane on a stand and the laser (or collimator) is installed on a precision bench that can translate 4 inches or more accurately (e.g., on the table of a milling machine).

The laser is first aligned perpendicular to the alignment mirror (by causing the reflected beam to be directed back into the laser aperture). A simple aperture plate having an opening diameter equal to that of the laser beam is placed immediately in front of the laser aperture. If an aperture plate is not readily available, a piece of cardboard which has been perforated to provide the desired hole diameter may be used. The reflected beam will be slightly diverging, yielding a halo on the aperture plate around the aperture when the laser and the alignment mirror are correctly aligned. The laser (or collimator) is then translated such that the primary mirror is illuminated (or viewed) close to the periphery of the inner telescope tube. The location of the laser reflection in the image plane of the telescope is examined next. This is accomplished by inserting a disc inscribed with concentric rings in the image plane and observing which target ring is illuminated by the laser. The target should be symmetrically trimmed to a size that can be press-fitted into the reticle ball bearing under the clamp in Figure 5. By articulating the mirror cell shown in Figure 1 via the four socket head cap screws (see Figure 4) the reflection is positioned such that it falls on the center of the target. Since the mirror cell has two degrees of freedom, the above procedure is repeated for a laser position which illuminates a portion of the primary mirror at the same radial distance from the mirror center, but

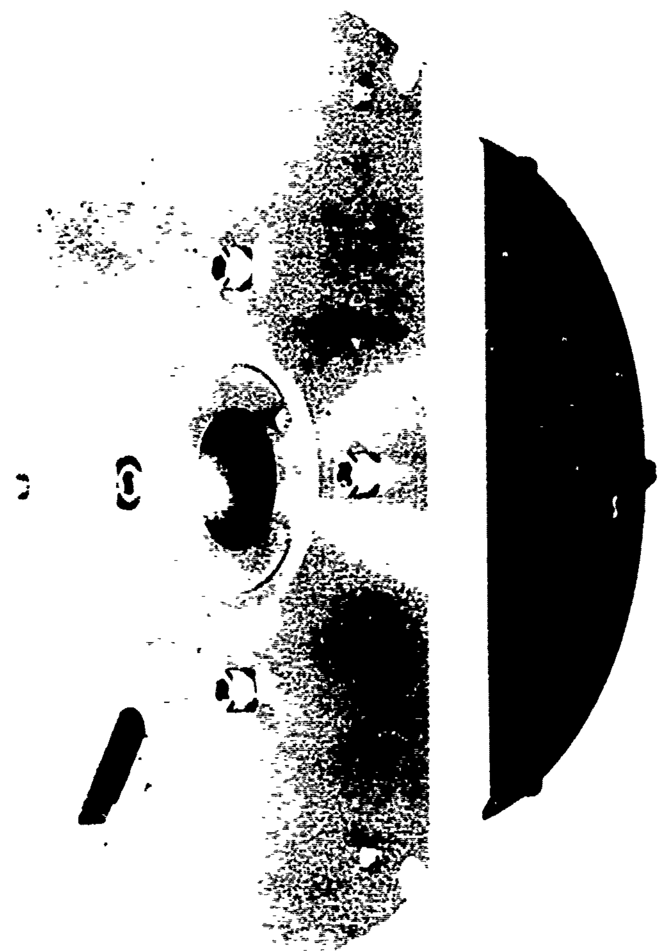

Figure 4. Mirror assembly.

at an angular position approximately 90° removed. The above procedure is repeated until proper alignment is achieved.

3. Installing the Photomultiplier Tube (see Figure 5)

The photomultiplier (PM) tube is supported in the inner telescope tube via rubber rings and clamped in place between the bearing clamp and the PM tube clamp via a number of other parts. The PM tube is installed by first inserting the four rubber rings shown in Figure 5, the rubber front end spacer, the filter holder, the bearing and the bearing clamp. The bearing clamp is designed to be tightened using a spanner wrench. Before tightening, however, the orientation of the filter holder should be inspected to ensure that it is installed with the filter facing in as as shown in Figure 5 (this is required in order to provide full support to both sides of the front end spacer). The PMT may now be inserted into its place; it is recommended that some silicone grease be applied to the PM tube in order to facilitate the tube sliding through the rubber support rings. Finally, the back end seal is installed, back end spacer, and the PM tube clamp nut as shown in Figure 5 thereby completing the installation procedure for the PM tube proper.

At this point in the installation, the PM signal lead can be mated to the high voltage electronics unit (HV unit). The HV unit should first be assembled as described in Section 5 below. With the HV unit detached from the telescope front plate and with the cover to the HV unit removed insert the PM signal lead through the appropriate hole in the HV assembly base plate. Next, mate the connector at the end of the signal lead to the connector on the assembly which contains the electrometer amplifiers and VCO units. The mating of the connectors is facilitated by first detaching this assembly from the structure brackets. Reinstall the electrometer VCO assembly and attach the HV feedthrough portion of the PM signal lead to the base plate (including the "O" ring seal). Finally, attach the cover to the HV unit and mount the HV unit to the front plate.

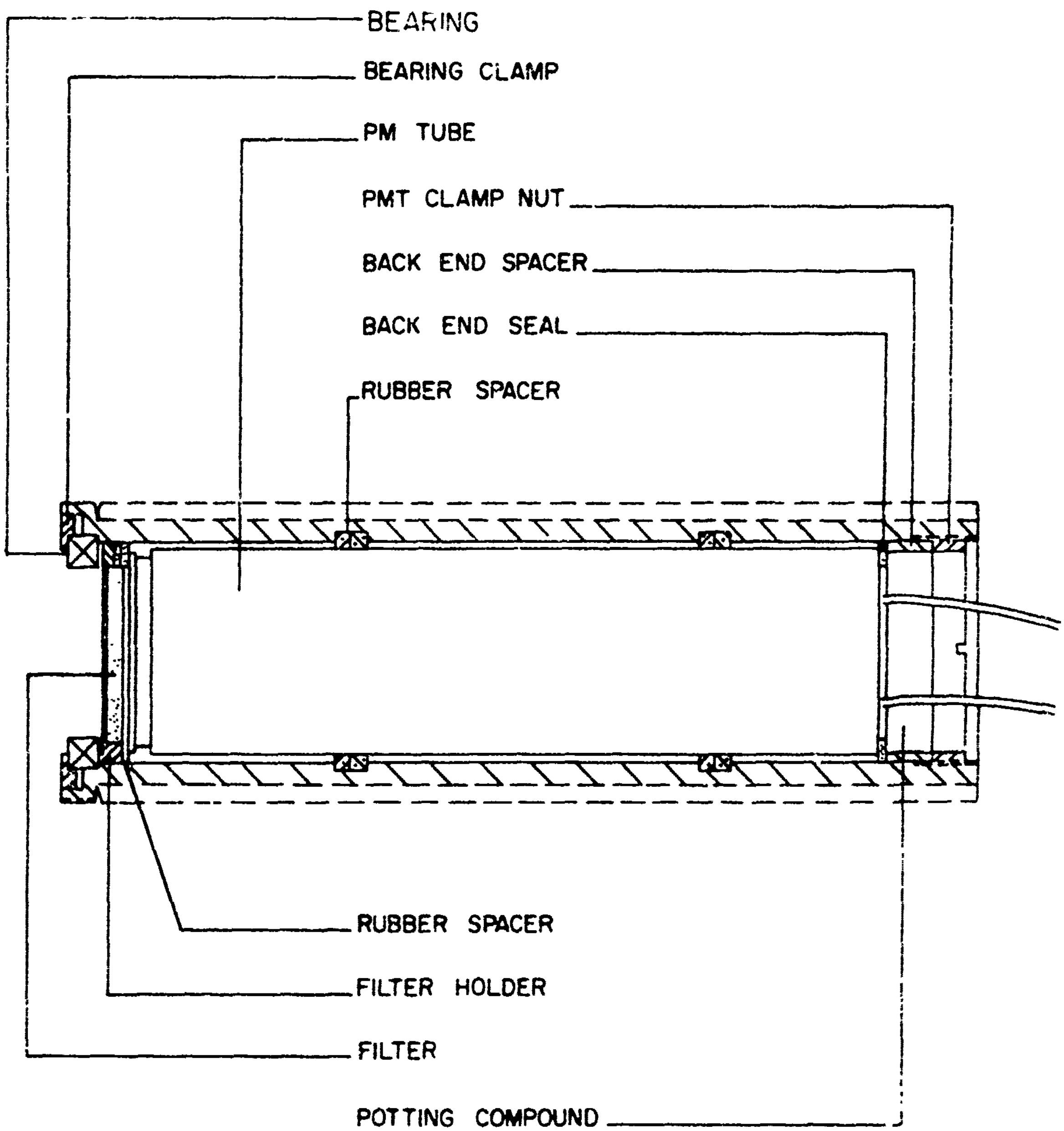

Figure 5. PM Tube Assembly

To disassemble a PM tube, the signal lead is first disconnected and the above mentioned steps are followed in reverse. Then the PM tube clamp nut is removed and two #4-40 screws each 1-1/2 inches long are installed in the two holes in the base of the PM tube. The tube is extracted from the inner telescope tube by pulling on these two screws.

4. High Voltage Electronics Unit (see Figure 6)

The high voltage electronics unit (HV unit) is maintained at atmospheric pressure to prevent arcing and corona when the photometer is operating in a vacuum environment. Each time the cap of this fitting is installed the thread of the fitting should be provided with a suitable sealant. When assembling the HV unit, the bottom card is to be installed first as shown in Figure 7, cards #2 and #3 are to be attached to the spacers first and then they are installed on the brackets. The electrometer conditioning circuitry and VCO assembly shown in the top one third of Figure 7 is to be fully preassembled including the aluminum cover (center item in Figure 6) before it is attached to the structure brackets. It should be pushed forward as shown in Figure 7 as much as possible while tightening the mounting screws.

5. Miscellaneous Remarks

Each photometer is provided with a monitor mirror as indicated in Figure 1 and underneath the right cap in Figure 2. It is exposed to the same environment during the history of each photometer as the primary mirror and is therefore a measure of the status of the reflective surface of the latter. It is installed and removed by simply screwing the mirror holder into or out of the front plate. Each photometer is also provided with a functional check source (CAL LAMP) as shown in Figures 1 and 2. This source emits energy at the appropriate optical wavelengths on remote command or upon command from an on-board timer. It is attached to the bottom plate of the mirror assembly via two screws and via a permanent harness to the low voltage electronics unit.

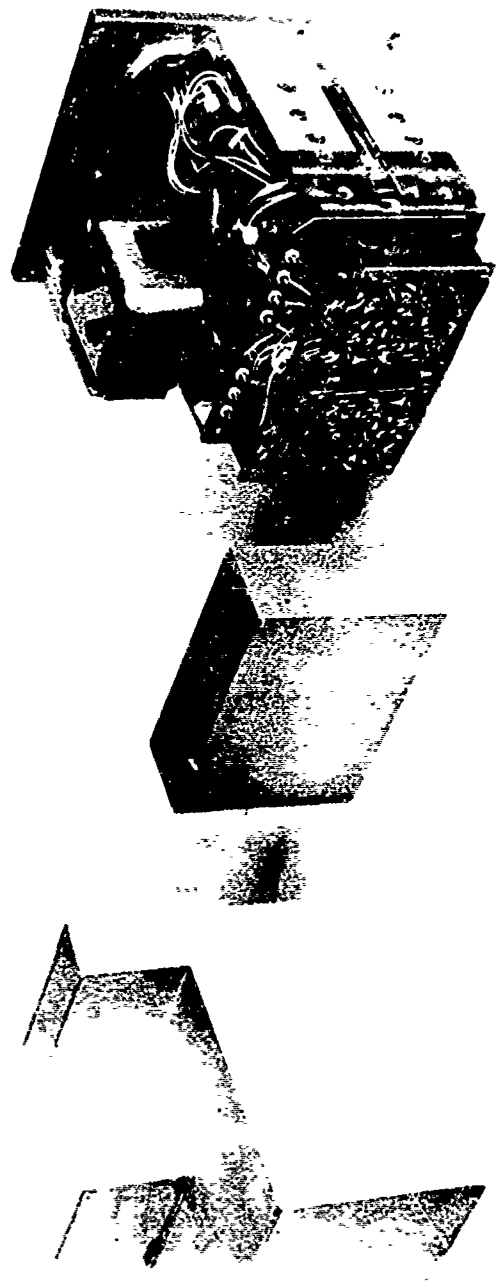

Figure 6. High voltage electronics unit.

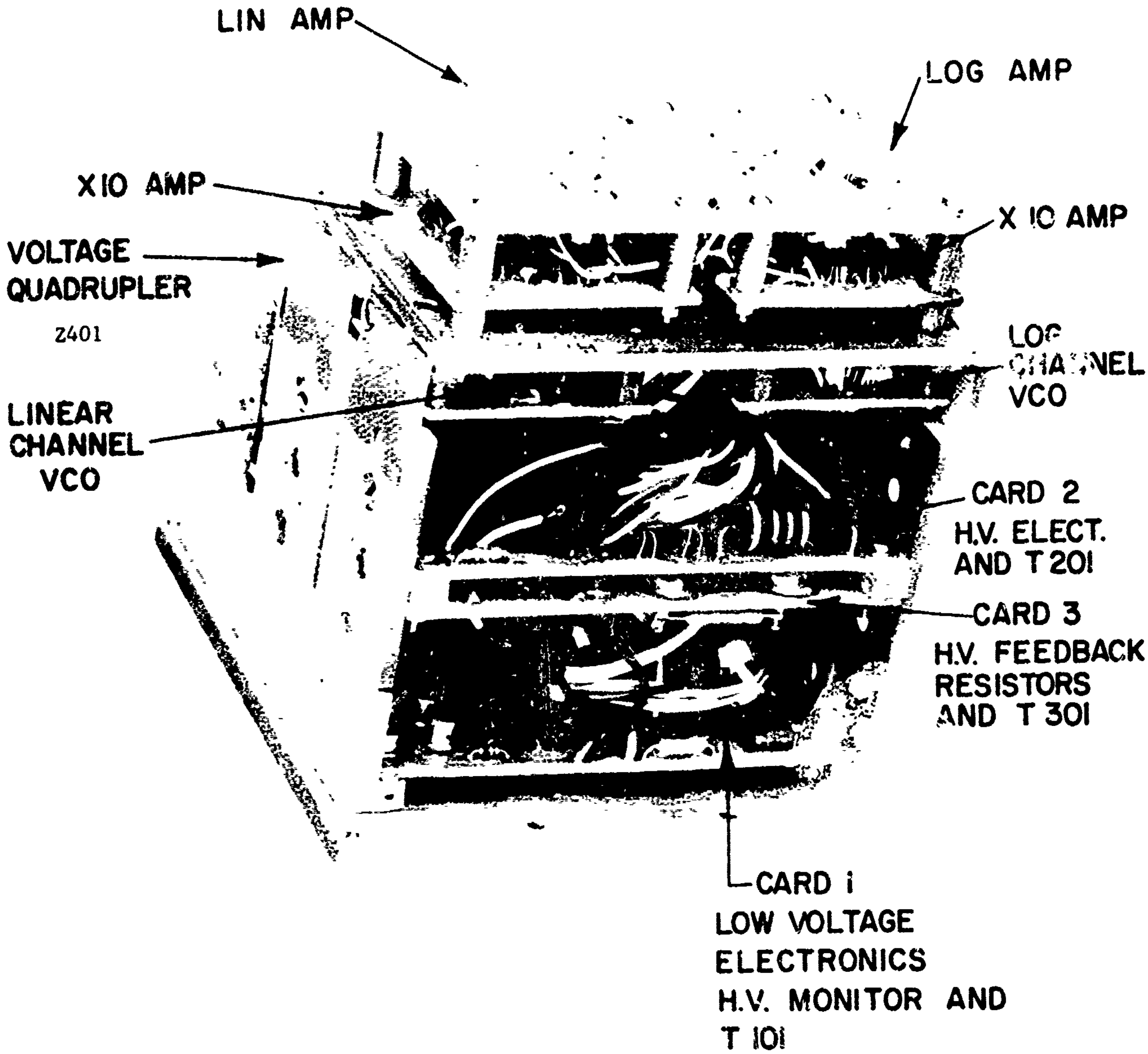

Figure 7. Component locations in high voltage electronics unit.

The low voltage electronic unit shown in Figure 8 is attached to the bottom plate only during transit. When installed in the payload, this unit is attached to the payload structure and is mechanically separate from the main photometer assembly.

C. OPTIONAL ACCESSORY ATTACHMENTS

1. Rotating Reticle

Each photometer can be provided with a rotating reticle. This consists of a reticle wheel which is driven via a mylar belt by a two phase (capacitor phase shift network) motor and is provided with a position sensing device.

The reticle wheel shown in Figure 9 is pressed into the bearing shown in Figure 5; however the bearing clamp is assembled between the reticle wheel and the bearing prior to pressing the latter two together. The bearing clamp is installed onto the inner telescope tube as described previously (Section II.B.3) but now the two holes in the reticle wheel must be lined up with the spanner wrench slots in the bearing clamp to facilitate inserting the spanner wrench.

The position of the drive motor is adjusted with shims such that the belt will run properly. When interchanging the drive motor for a new one the same sets of shims should be installed in the same places.

The mylar drive belt must be handled very carefully during installation. It should be layed with its full width over the motor shaft prior to working the belt onto the reticle wheel.

The reticle wheel is provided with a soft iron strip along 180° of its periphery and its orientation is determined by a magnetic sensing element as shown in Figure 9. The element is installed as shown in Figure 9 and aligned with respect to a suitable lateral reference with the aid of a protractor to assist in interpreting the field data in terms of the local horizontal.

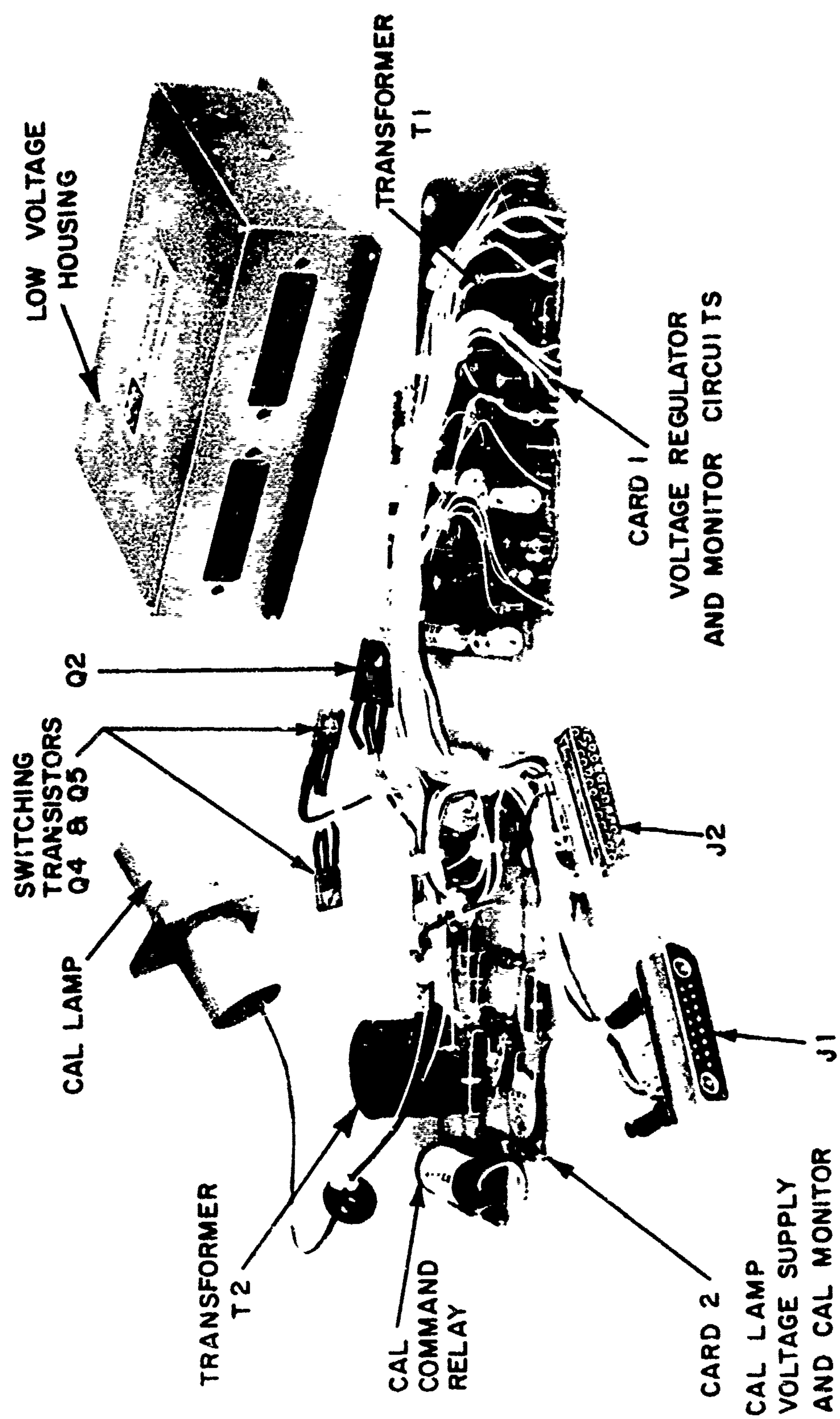

Figure 8. Exploded view of low voltage electronics unit.

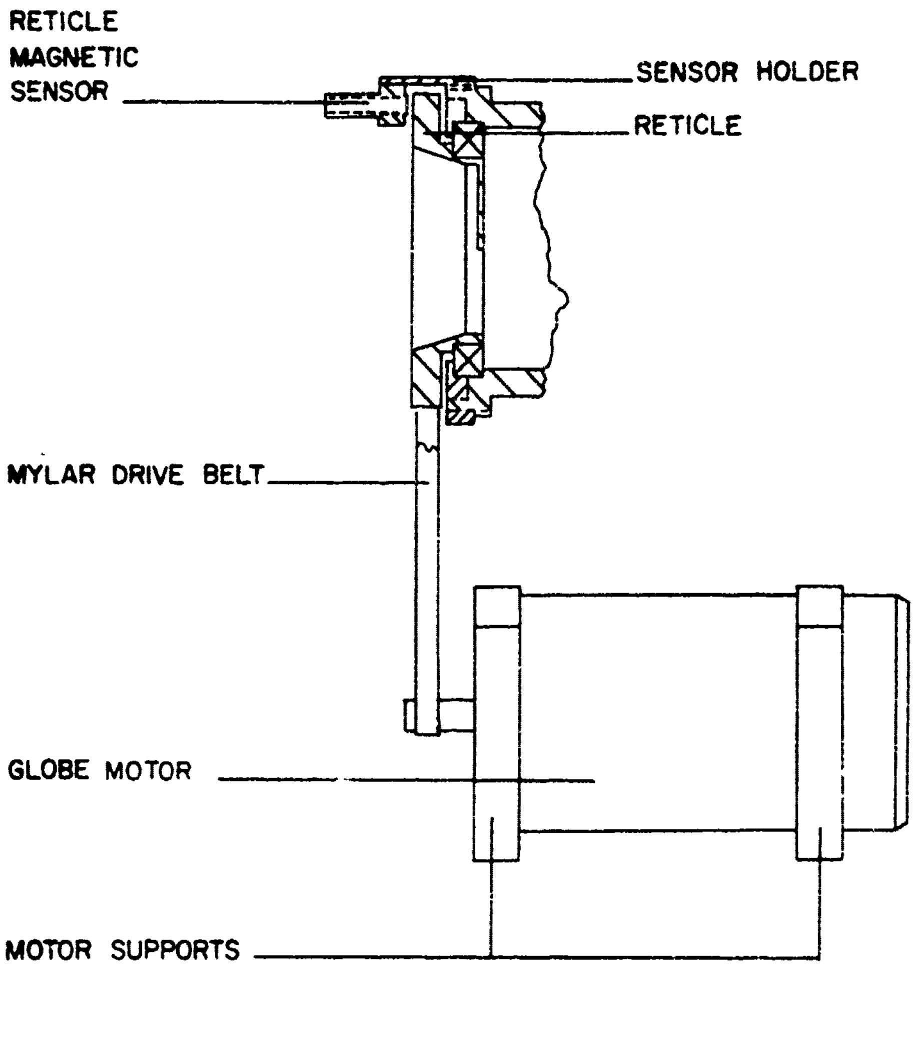

Figure 9. Reticle Assembly

2. The Fixed Optical Filter

An optical filter is retained in the filter holder (as shown in Figure 5) and installed immediately in front of the photomultiplier tube. When installing a filter, the PM tube clamp nut, (shown in Figure 5) is first backed off one turn, then the bearing clamp, bearing and filter holder are removed; the filter is then inserted into the filter holder and is reassembled as described in Section II.B.3.

3. The Movable Optical Filter (see Figure 10)

Each photometer can be provided with the "flip" filter assembly shown in Figure 10. The attachment consists of a filter which is installed on an arm driven by a torque motor which alternately inserts and withdraws the optical filter from the image plane. The assembly is provided with position sensing devices.

The filter is retained in the arm with rubber pads and the heads of three screws. The mass of the filter arm assembly is counterbalanced by a weight and this balance has to be rechecked when the filter is interchanged. The filter arm is electrically driven both to the "in" position (filter is present in the focal plane) and to the "out" position. Mechanical stops establish the terminal positions of the filter. One step in the preflight checkout procedure should include an inspection of the mechanical stop for the "in" position in order to ensure that it has not shifted from its intended position. (This is established by examining the position of the filter with respect to the inner telescope tube). The filter arm position sensors consist of two micro switches. Their actuation point should be adjusted each time the flip filter assembly is installed on the photometer such that the "in" and "out" positions are properly sensed.

When replacing the drive motor, care should be taken that the rotor is never removed from the stator because removing it will break the magnetic circuit. This would result in a permanent decrease in magnetic field strength and consequently in a reduction of output torque. The stator is retained in a housing and the rotor is

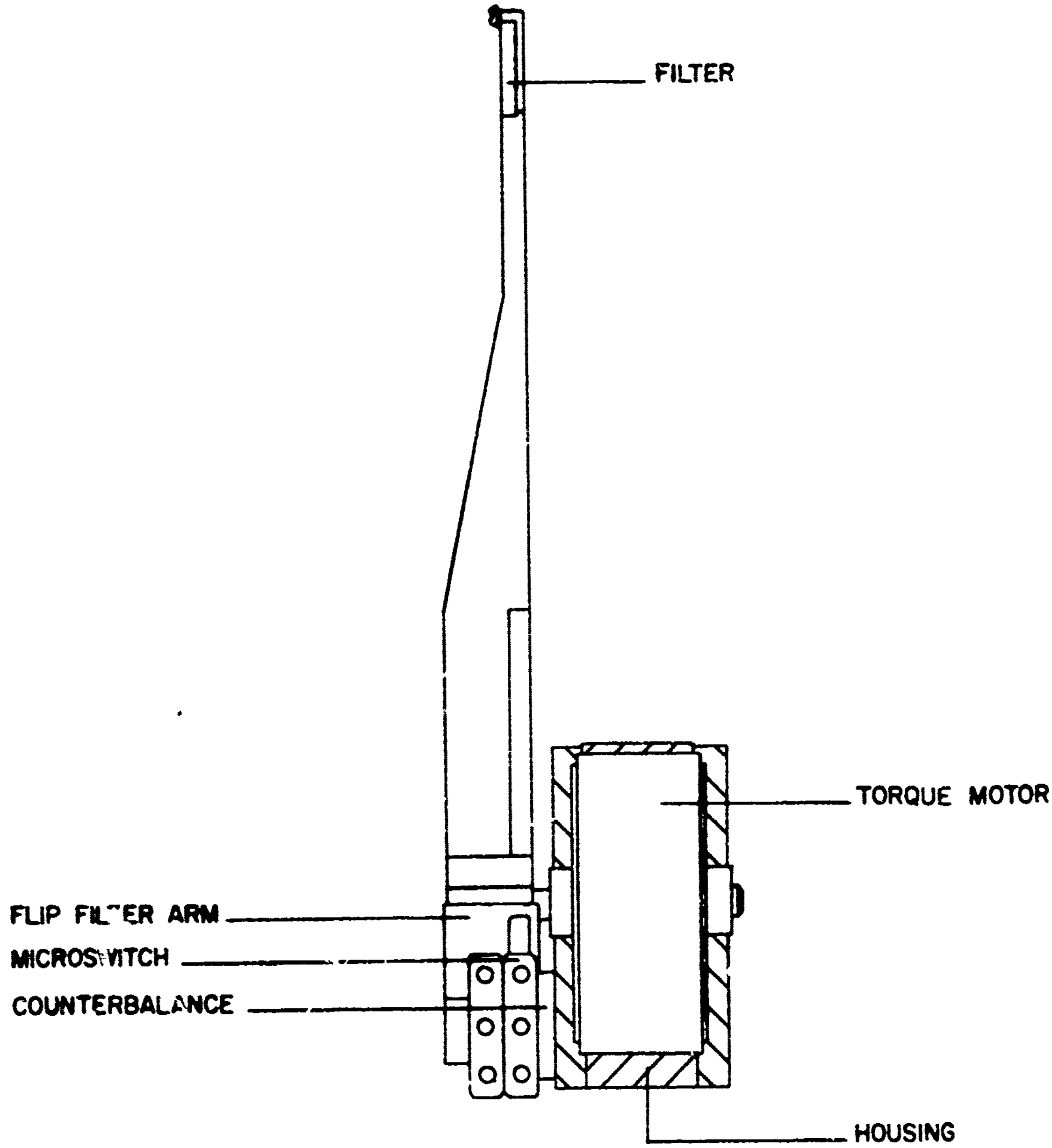

Figure 10. Flip Filter Assembly

held between two end plates. It is to be noted that the same shaft spacers are to be installed in a replacement motor as are present in the old motor.

D. OPTICAL PARAMETERS

The optical system consists of a series of baffles, an aperture stop, an f/1 mirror, and a field stop. A typical baffle is shown and stop are shown in Figure 1. The diameter of the aperture stop is 11.2 cm yielding a net collecting area of 82.5 cm^2 when the obscuration of the PM tube mount (4.45 cm diameter) is taken into account.

The f/1 spherical mirror was ground from a 12 cm diameter pyrex blank with the front surface having a 22.4 cm radius of curvature yielding an 11.2 cm focal length. It has a centrally located cored hole of 2.5 cm diameter to accomodate the calibration lamp described previously in Section II.B.5. It was aluminum coated and overcoated with MgF_2 or SiO as appropriate for the spectral region of interest.

The cathode area of the PM tube, which has a diameter of 2.5 cm, constitutes an effective field stop. In conjunction with the given focal length this yields a nominal system field of view (FOV) of 12°. Plots of the actual FOV, for each instrument, showing the roll off of the edge and the attenuation in the wing are included in Appendix A.

III. ELECTRONIC DESIGN

A. SUMMARY DESCRIPTION

The electronic design of the photometer modules is shown in simplified block diagram form in Figure 11. The electronics circuitry is contained in two major modules: (1) the low voltage electronics unit which is designed to operate exposed to the ambient upper atmospheric pressure environment, and (2) the high voltage electronics unit which is contained in a sealed housing ideally maintained at a pressure of one atmosphere. The low voltage electronics provides 60 Hz a-c drive power for the reticle motor, d-c voltages to the calibration lamp, and regulated d-c power for the various operational amplifier circuits which are used in the system. The high voltage electronics contains the high voltage power supply for the photomultiplier tube and also contains the electrometer amplifiers and voltage controlled oscillators (VCOs) which are used to process the output of the photomultiplier tube.

Except for the frequency allocations of the VCOs, the same basic electronic design is used in all photometers. All photometers contain circuitry which will provide reticle motor drive and an in-out filter torque motor drive capability even though these elements are optional in each photometer. The alphanumeric identification of the PM tubes, and the serial number designations for the electronic subsystem components are listed in Table I. The table also indicates VCO frequency assignments and optical filter assignments. The channels which contain the rotating reticle and the in-out filter accessories are identified in the same column which lists the optical filter assignments. The resistance value listed under the PM tube designations indicate the value of resistance used between adjacent dynodes of the multiplier.

A detailed description of the electronics circuitry is contained in the following discussions.

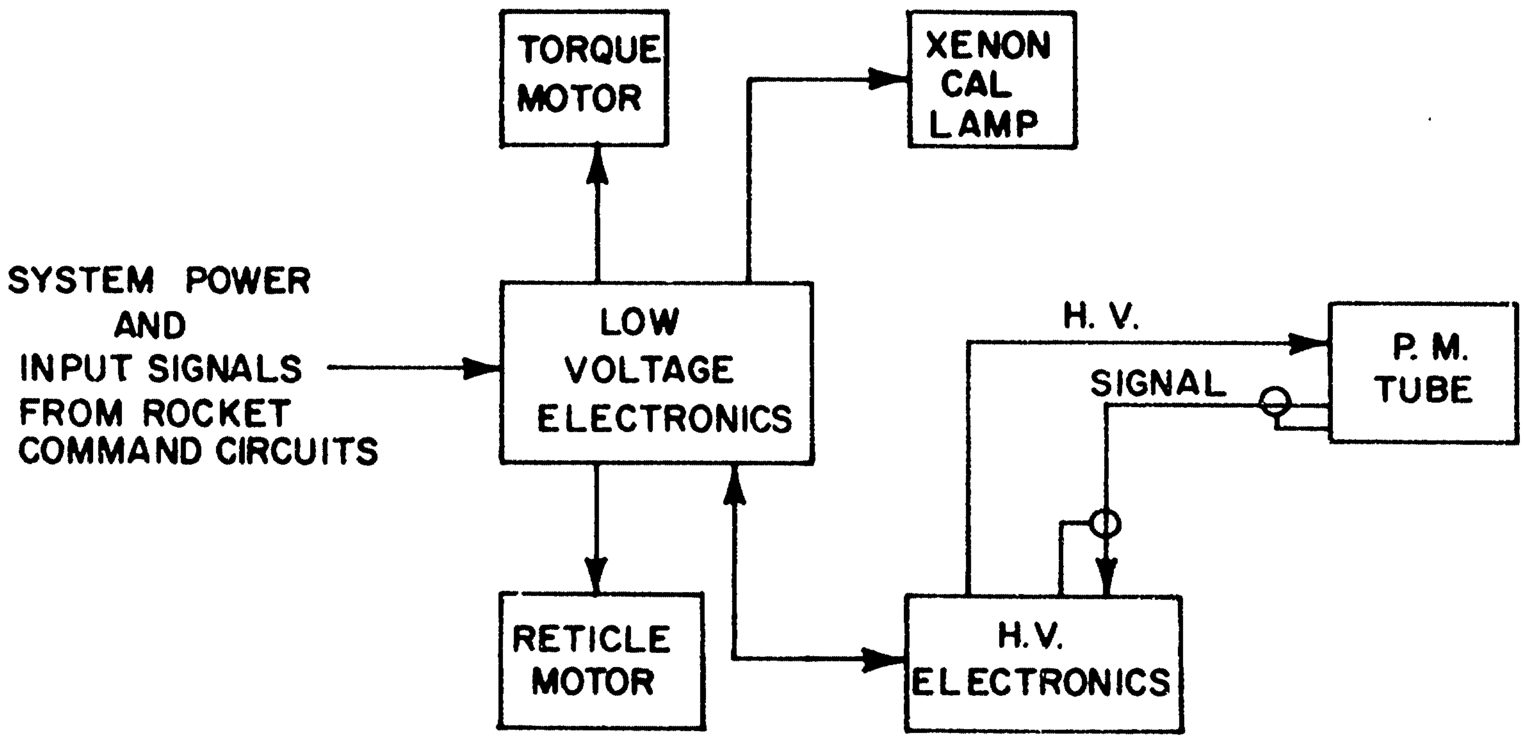

Figure 11. Chaser photometer major electronic components.

TABLE I

ORIGINAL COMPONENT ASSIGNMENTS FOR CHASER PHOTOMETERS (SEE NOTE 1)

Serial Number of System	PM Tube and Dynode Resistance	Low Voltage Electronics	High Voltage Electronics			Description
			Module Designation	Lin. VCO	Log. VCO	
SN #1 (Channel) Photometer #3	B2 3.9 meg	SN #1	SN #1	#11 14.5 KHz	#6 5.4 KHz	Corion Filter #1 Mirror #5
SN #2 Photometer #1	A3 1 meg	SN #2	SN #2	#7 7.35 KHz	#1 3 KHz	In-Out Filter Mirror #1
SN #3* Photometer #2	A4 1 meg	SN #4	SN #3	#9 10.5 KHz	#4 3.9 KHz	Seavom Filter #172 Reticle Motor Mirror #2
SN #4 Photometer #3	B3 3.9 meg	SN #3	SN #4	#12 14.5 KHz	#5 5.4 KHz	Corion #2 Mirror #6
SN #5 Photometer #1	A1 3.9 meg	SN #5	SN #5	#8 7.35 KHz	#2 3 KHz	In-Out Filter Mirror #4
SN #6 Photometer #2	A5 1 meg	SN #6	SN #6	#10 10.5 KHz	#3 3.9 KHz	Seavom Filter #173 Reticle Motor Mirror #3

TABLE I (continued)

NOTE 1

In April 1972 the refurbishment effort performed after the second flight resulted in the following assignment changes:

1. <u>System SN #1</u>
   a. B1 was substituted for B2.
   b. Mirror #5 was stripped and recoated.
   c. Corion filter #3 was substituted for Corion filter #1.
   d. Low voltage electronics module SN #2 was substituted for low voltage electronics module SN #1.
2. <u>System SN #2</u>
   a. A7 was substituted for A3.
   b. Mirror #1 was stripped and recoated.
   c. Low voltage electronics module SN #1 was substituted for low voltage electronics module SN #2.
3. <u>System SN #3</u>
   a. A6 was substituted for A4.
   b. Mirror #2 was stripped and recoated.
   c. Seavom filter #250R was substituted for Seavom filter #172.
4. <u>System SN #4</u>

   no change
5. <u>System SN #5</u>

   no change
6. <u>System SN #6</u>
   a. Seavom filter #270 was substituted for Seavom filter #173.
   b. Mirror #3 was stripped and recoated.

B. LOW VOLTAGE ELECTRONICS

1. Block Diagram Description

The basic circuit elements contained in the low voltage electronics are shown in block diagram form in Figure 12. The low voltage electronics unit accepts 28V d-c system power and various command signals from the rocket control circuitry, and, as discussed above, provides a-c motor power, d-c power to the calibration lamp, and d-c regulated power to the operational amplifier circuits.

The +28V supply voltage is first applied to a reverse polarity protection circuit and then to the pre-regulator circuit which provides a +23V regulated output. The regulated +23V output provides power to the system d-c to a-c converter and to a 60 Hertz oscillator. The system inverter operates at approximately 13 KHz and produces d-c output voltages at nominal levels of +210V, +900V, and -700V. A pair of 90V p to p a-c output voltages are delivered to transformer T2 in the high voltage electronics unit. The +210V output is used to power the amplifier which provides the 60 Hertz a-c drive voltage to the reticle motor. A mylar belt is used to couple the motion of the reticle motor output shaft to the reticle rim. The direction of rotation of the reticle is clockwise as observed facing the PM tube cathode.

The position of the reticle is monitored by a magnetic sensor which is placed near the rim of the reticle. The sensor is located on the side of the reticle nearest to the reticle motor and is in the plane which passes both through the center line of the motor shaft and the center of rotation of the reticle. A soft iron strip in the shape of a semi-circular ring is fastened on the reticle outer surface such that it is located in the 180° sector of the reticle which is masked (SN6) and unmasked (SN3). As the soft iron strip passes by the magnetic sensor, two reference pulses are produced in the sensor coil, one with negative polarity as the beginning portion of the strip passes by the sensor and the other with positive polarity as the end portion of the strip passes by the sensor. The sensor reference pulse output

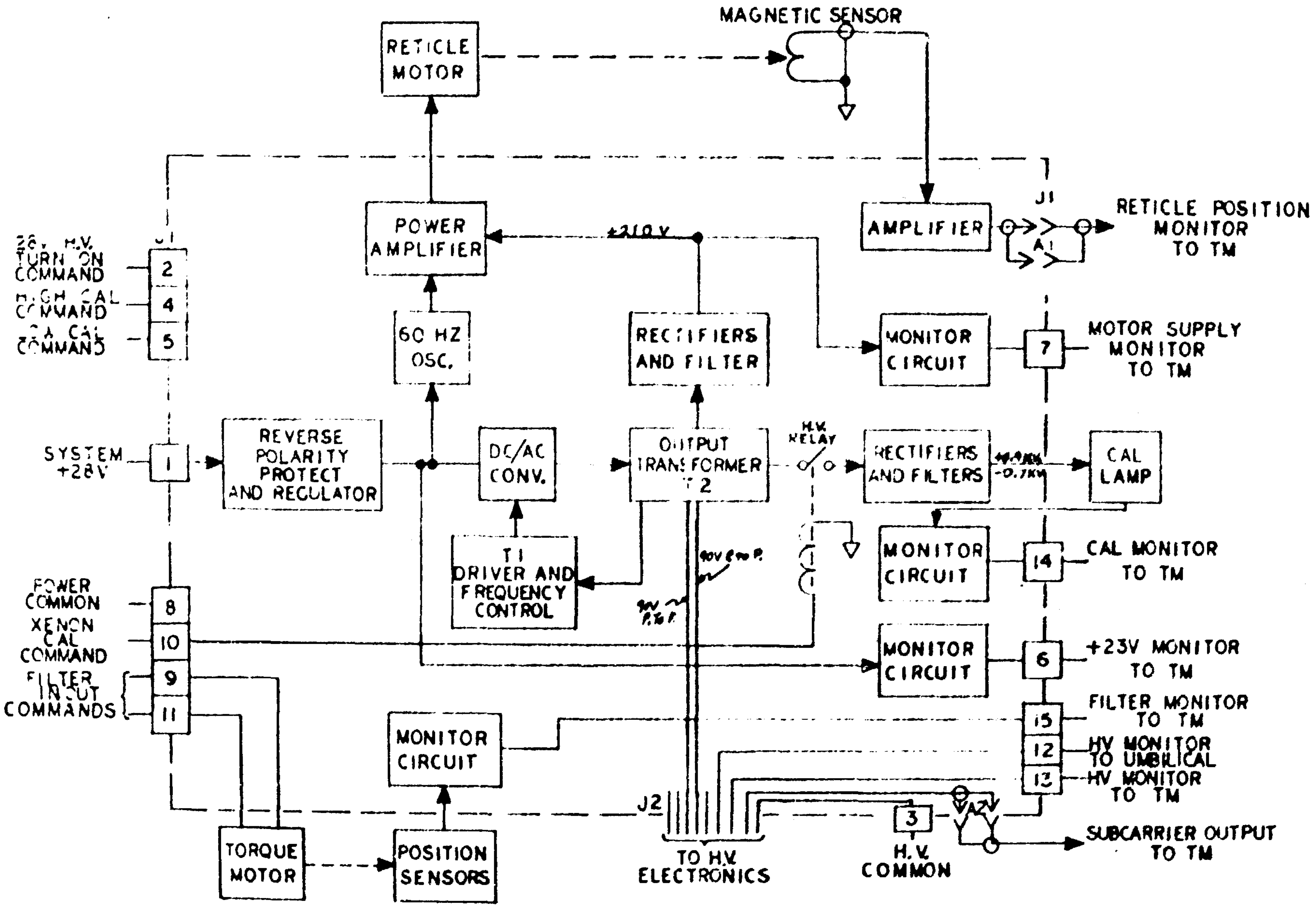

Figure 12. Low voltage electronics.

is amplified and provides an output to the rocket telemetry system to modulate one of the VCO modules. The d-c level of the reticle monitor signal is +2V nominal and the amplitude of both the negative and the positive output pulses is 1.5V peak. The reticle monitor signal is used as a phase reference signal during the data reduction process after a flight.

The +900V and -700V outputs of the inverter are generated whenever the high voltage relay is activated by the Xenon Cal Command signal. These voltages are applied to a small xenon discharge lamp which is used to produce an output level of light for the system confidence check. Normally, the xenon cal lamp is turned on by the rocket command circuits before and after the measurement interval.

Monitor output signals are generated using precision resistor dividers which sample key signal and supply voltages. The attenuation of each divider is such that the monitor output signal levels are confined to the standard telemetry range of 0 to +5V. The monitor outputs are delivered primarily to the commutator portion of the telemetry system. The pertinent chracteristics of the monitor signals are summarized in Table II. The first four are generated in the low voltage electronics, while the last one is generated in the high voltage electronics.

Two push pull a-c inverter output signals are applied to T2 in the high voltage electronics unit. These outputs, each of which has an amplitude of 45V p to p are used both to synchronize the operating frequency of the high voltage power supply with the operating frequency of the inverter in the low voltage electronics and to generate the isolated +16V and -16V d-c supplies for the circuits which process the anode output signals of the photomultiplier tube.

2. Schematic Description

A schematic representation of the low voltage electronics is contained in Figure 13. Input +28V d-c power at pin 1 of J1 is preprocessed by a voltage regulator consisting of Q_1, Q_2 Q_3, voltage

A

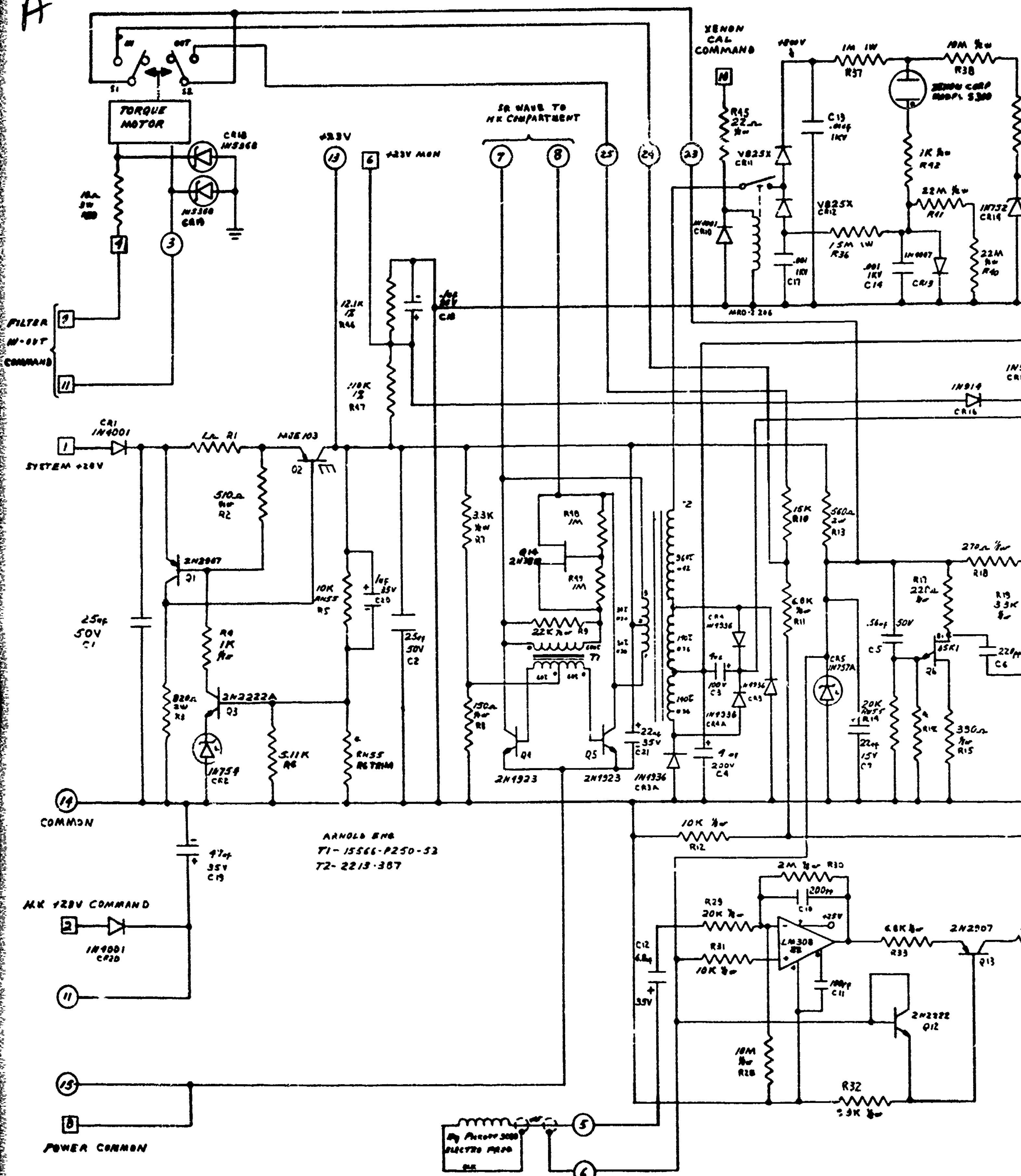

Figure 13. Motor and I

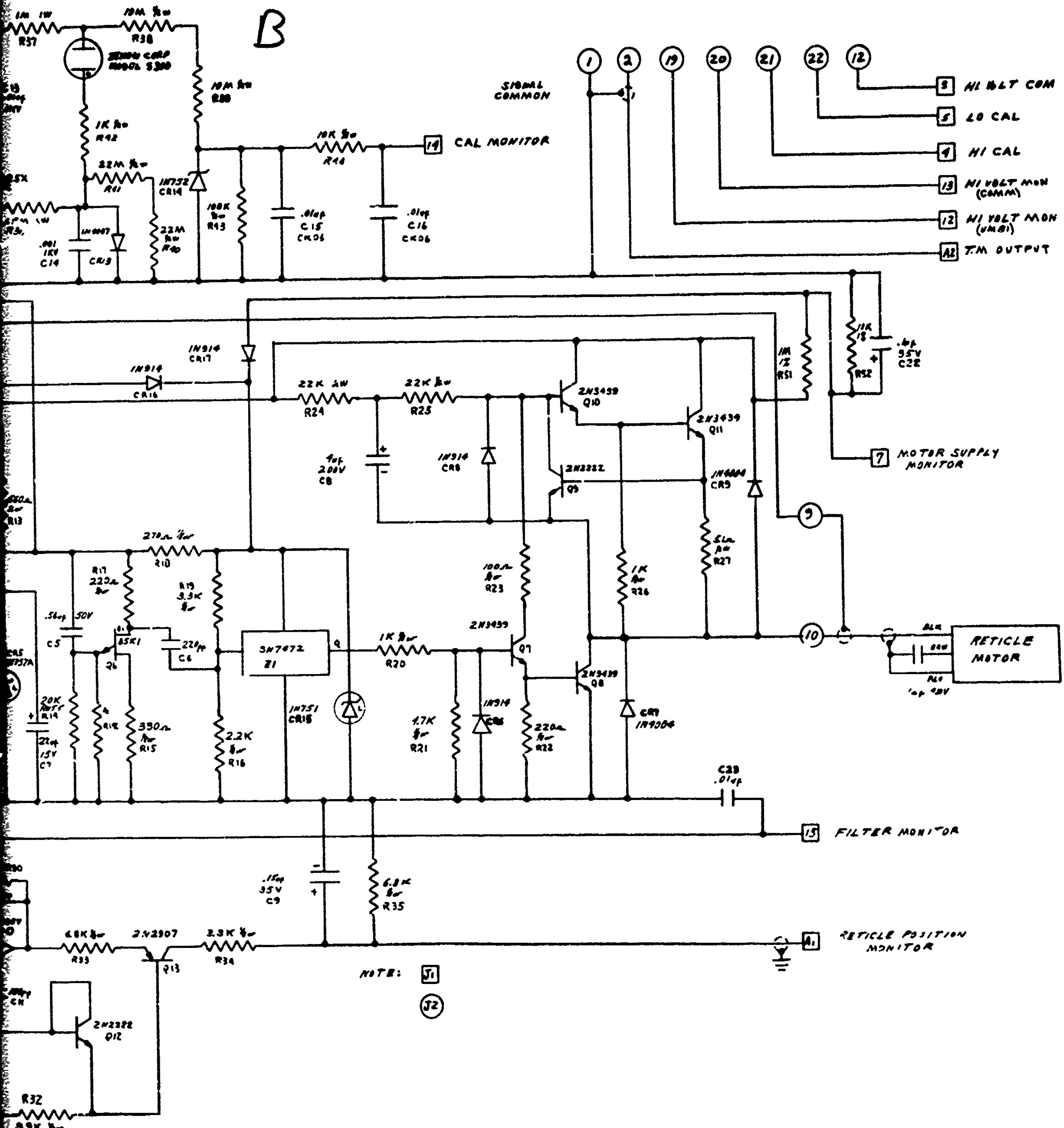

ure 13. Motor and Lamp Devices

TABLE II

PHOTOMETER MONITOR OUTPUTS

Monitor Parameter	Scale Factor Relationship	Signal Characteristics
Regulated +23V	$E_{regulated} = 10\ E_{monitor}$	23V d-c nominal output
Motor supply	$E_{motor} = 100\ E_{monitor}$	210V d-c nominal output
Filter position		5.2V nominal represents "in" 2.7V nominal represents "out" 0V represents indeterminate position between "in" and "out"
Cal lamp condition	$E_{lamp} \approx 200\ E_{monitor}$	0V indicates that lamp supply not active +2.5V nominal indicates that lamp is firing normally 3.5V nominal indicates that lamp voltage is on but lamp is not firing
High voltage		
a. TM monitor	$E_{HV} \approx 1000\ E_{monitor}$	+2.5V to +3.6V depending on high voltage setting
b. Umbilical monitor	$E_{HV} \approx 600\ E_{monitor}$	4V to 6V depending on high voltage setting

reference diode CR2 and associated circuitry. Transistor Q_1 operates both as an amplifier for the output of Q_3, and also as a current regulator which is activated by the voltage drop across current monitor resistor R1. For any overload condition, in which the resulting voltage drop across R1 approaches about 0.7V, transistor Q_1 will conduct and shunt out the current applied to the base of Q_2 thereby overcoming the output of Q_3. This action serves to limit the maximum collector current through Q_2 to a value given approximately by 0.7/R1 amperes. In the absence of an overload the regulated voltage at the collector of Q_2 will be +23.0V nominal.

The 23.0V regulated output is used to provide power to the d-c to a-c converter which consists of switching transistors Q_4 and Q_5, drive transformer T1 and output transformer T2. Transformer T1 is wound on a tape-wound toroidal core whose square loop magnetization characteristics are used to determine the operating frequency of the converter. Two low voltage outputs of T2 are applied to a full wave bridge rectifier which is used to obtain d-c output voltages of +210V and +105V. These outputs provide d-c power to the reticle motor power amplifier which consists of Q_7, Q_8, Q_9, Q_{10}, Q_{11} and associated components. Transistor Q_9 and resistor R27 are used to provide short term overload protection in the event that the motor windings are inadvertently short circuited during tests.

The 120 pps reference frequency for the motor drive amplifier is obtained from the unijunction oscillator, transistor Q_6. The negative output pulses of Q_6 are frequency divided by flip flop, Z1, to obtain the required 60 Hz square wave output signal. The effects of power supply variations on oscillator frequency are minimized by the use of a zener regulator, CR5 which provides a stable 9V source of power for Q6. A second zener diode regulator CR15 is used to maintain the flip flop supply at +5V d-c.

As discussed previously, a magnetic sensor is used to monitor the position of the spinning reticle. Capacitor C12 is used to

a-c couple the output of the sensor to the LM308 operational amplifier, Z2. Because the d-c output level of Z2 is +12V, a level changer consisting of Q_{12}, Q_{13} and associated resistors is used to translate the amplifier output to the standard telemetry range of 0 to +5V. The d-c output level of Q_{13} is +2V nominal in order that the reticle monitor output pulses of +1.5V peak and -1.5V peak will not cause the net output of Q_{13} to go below 0V or above +5V.

DC output voltages for the calibration lamp are obtained by rectifying the output at the high voltage tap of T2. Whenever the xenon cal command signal is on, the high voltage relay K1 will close and couple the high voltage output of T2 to rectifier diodes CR11 and CR12. The output of CR11, nominally at +900V, will be applied to the anode of the calibration lamp through a current limiting resistor R37. Similarly, the output of CR12, nominally at -700V, will be applied to the cathode of the lamp through resistor R36.

When the lamp fires, the lamp voltage drop will decrease to approximately 500 volts and the cathode will clamp to ground potential through diode CR13.

The calibration lamp circuit is monitored by the attenuator consisting of R38, R39 and R43. The output of this attenuator, the cal monitor output, will be 0 volts with no xenon cal command signal and either +3.7V or +2.5V with the cal command applied. A +3.7V output indicates a "no fire" condition for the cal lamp. The +2.5V output indicates the normal "on" condition of the cal lamp and should be present whenever the cal command is activated.

A metal shield with a pinhole was made to slide over the front of the lamp to bring lamp emission into the readable range of photometers.

C. HIGH VOLTAGE ELECTRONICS

1. Block Diagram Description

The high voltage electronics circuitry is shown in detailed block diagram form in Figure 14. As is evident from the figure,

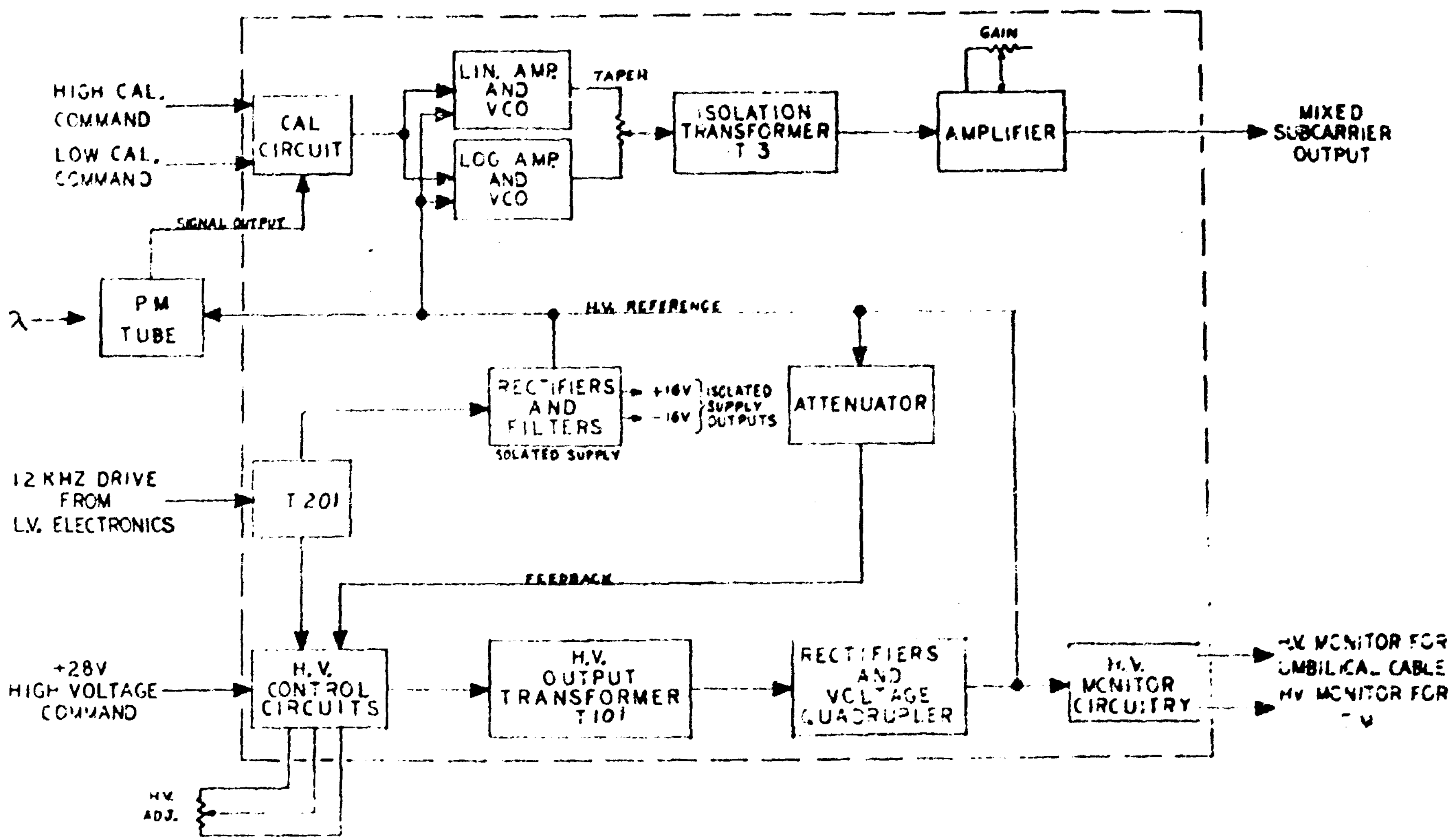

Figure 14. High voltage electronics.

the high voltage electronics circuitry consists of two basic parts; one part which contains the high voltage producing and monitoring circuits, and a second part which contains the signal processing circuitry.

The high voltage circuitry is turned on by the +28V high voltage command signal which activates the high voltage control circuits. An externally located high voltage adjust potentiometer indirectly controls the d-c supply voltage applied to the center tap of T101. The d-c input power to T101 is converted to an a-c output voltage by a pair of high level switching transistors. As discussed previously, synchronization with the low voltage electronics inverter frequency is ensured by transformer T201 which couples a small portion of the a-c output of the inverter in the low voltage electronics unit to the bases of the switching transistors. The a-c output of T101 is converted to d-c by a voltage quadrupler rectifier circuit which produces the high voltage output for the PM tube. Negative feedback from a tap on the high voltage monitor to the control circuitry maintains a high degree of regulation.

An auxiliary output of the high voltage attenuator is processed by the high voltage monitor circuitry which provides two d-c monitor output signals. The lower level output consists of an 0.9V to 3.6V d-c output corresponding to high voltage values of 900 to 3600V. This output is provided to the telemetry commutator as an in-flight indication of high voltage. The second output operating at the somewhat higher output of 1.5V to 6.0V for the same 900V to 360V range of high voltage values is direct wired to the control console along with the other umbilical output lines. The high voltage monitor signals are measured with a digital voltmeter at the console and can be converted to the actual high voltage output with an accuracy of $\pm$ 0.2 percent. For the first six photometer instruments delivered under the CHASER program, the high voltage supplies were set for d-c outputs which were in the range of +2400 volts to +3600 volts.

Isolated d-c outputs of +16V and -16V are obtained by rectifying the a-c output of the specially insulated output winding of

T201. A simple active low pass filter at the output of each d-c output maintains output ripple to values of about 10 mV p to p or less. These low values of output ripple are necessary to ensure that fluctuation in the output of the isolated power supply will not induce significant displacement currents at the input of the electrometer amplifiers.

The signal processing circuitry for the PM tube output consists of a calibration circuit (composed of two relays, two precision resistors, and a zener regulated voltage source), a linear and logarithmic electrometer amplifier channel, two VCOs (voltage controlled oscillators), one for each channel, a signal isolation transformer, T301, and an output amplifier. Under normal operation, the output of the PM tube is directly connected to the linear and logarithmic amplifiers.

The amplification of PM anode output current is optimized by the use of a resistor isolation network at the inputs of the linear and logarithmic electrometer amplifiers. This network is designed such that 5/6 of the anode current will be applied to the input of the more sensitive linear electrometer amplifier and the remaining 1/6 of the anode current will be applied to the input of the logarithmic electrometer. For low level signals, signal processing of the linear channel can be further optimized during post flight data analysis by applying the recorded output of the linear channel to appropriate linear filters which could be used to reject statistical and other noise components. During playback of the recorded data several runs can be made using various filter settings in order to determine the best filter match for the data. When the best match is established, the actual data reduction could then be made using the filter bandwidth which corresponds to this best match condition.

For the logarithmic amplifier, linear filtering cannot be directly performed without the risk of introducing significant rectification errors. This is particularly true for signals which contain large fluctuations. Therefore, if frequency filtering is required for the logarithmic channel, the logarithmic signals will first have to be translated to linear form. This would have to be performed

on the ground during data reduction, either by using specially designed hardware or by entering the data into a computer and using an appropriate computer program to perform the filtering mathematically. Fortunately, however, the logarithmic amplifier is designed to process only the upper range of anode output currents. In this current range, it is anticipated that the signal levels will be relatively stationary so that statistical noise and other components of system noise will represent only a small percentage of the output current.

The loss of about 17 percent of the available anode current for the linear channel represents the performance penalty which results from the use of the dual linear-logarithmic amplifier system. This is relatively insignificant when compared with the better signal processing capabilities of the dual range system. Furthermore, the dual linear-logarithmic system features superior accuracy over most of the range of PM tube anode currents which are of interest.

In order to minimize rectification errors in the logarithmic amplifier channel which, as discussed above, could arise as a result of signal fluctuations, a modest input filter is used to reject frequencies above 230 Hertz. This cutoff frequency is well above the range of signal frequencies which are of interest so that the use of this filter will not result in any significant degradation of the PM tube output signals.

The outputs of the linear and logarithmic amplifiers are applied to two voltage controlled oscillators whose outputs are combined at the input of isolation transformer T301. The output of T301 is referenced to telemetry ground and is further conditioned by an adjustable gain buffer amplifier. The output of the buffer amplifier is a-c coupled to the telemetry modulation circuitry.

Upon receipt of the low cal command signal, the anode output of the PM is disconnected from the electrometer inputs and the low cal precision resistor together with the regulated voltage source is connected to the electrometer inputs so as to deliver a calibration current of 10^{-8} amperes. In a similar manner the high cal command also

disconnects the anode output of the PM tube and provides the higher calibration current of 3×10^{-6} amperes.

Because the d-c level of the PM anode may be as high as +3600V above telemetry common, the coils of the calibration relays cannot be directly energized by the calibration command signals. Instead, an optically coupled isolator having a 5000V insulation rating is used to translate the calibration commands to the high voltage level at which the isolated supply is referenced.

2. Schematic Description

A schematic representation of the high voltage electronics circuitry is illustrated in Figure 15. The high voltage power supply portion is presented in the lower half portion of the schematic. The upper half portion of the schematic illustrates the signal processing circuitry discussed above.

The d-c power for the high voltage power supply is supplied by the high voltage +28V command. The command signal first passes through reverse polarity protective diode CR20 in the low voltage electronic circuitry module and is then used to activate the high voltage regulator circuitry consisting of operational amplifier Z101, transistors Q101 through Q104 and associated resistors and condensers. Automatic startup is provided by a constant current generator consisting of FET transistor Q101 and current control resistor, R104. The output of Q101 is sufficient to drive zener diode CR101 into its breakdown voltage of 11.7V. The 11.7V output of CR101 serves as a reference input not only for Z101, but also for the high voltage adjust potentiometer.

The complete high voltage power supply consists of the high voltage regulator, switching transistors Q207 and Q208, transformer T101, voltage quadrupler network, Z401, and feedback resistors R301, R302 and R303. In operation the collectors of transistors Q207 and Q208 are alternately driven into full saturation by a balanced 13 kHz square wave output from T201. The 13 kHz input T201 is obtained

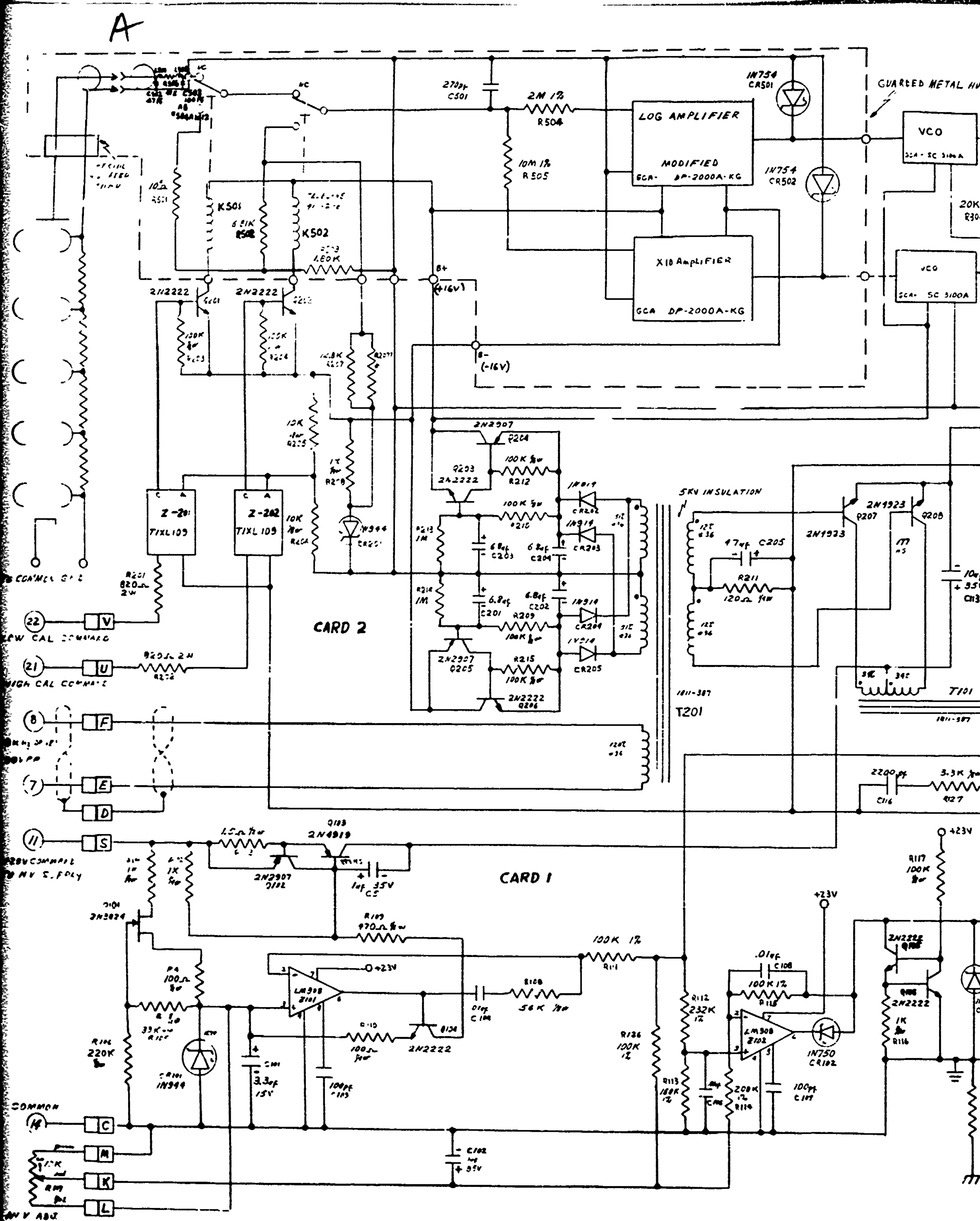

Figure 15. High Voltage Co

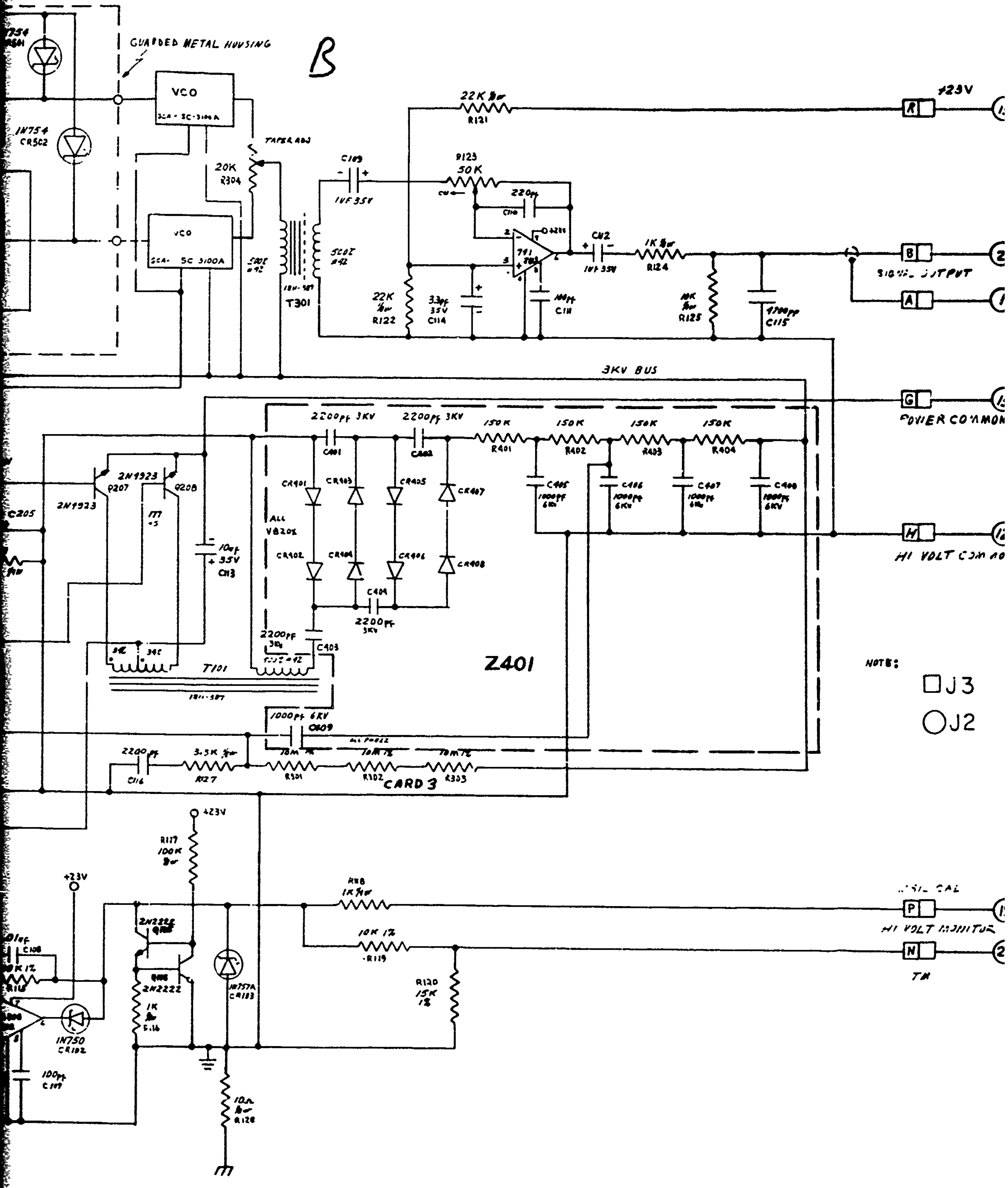

re 15. High Voltage Compartment

directly from the collector outputs of inverter transistors Q4 and A5 in the low voltage electronics unit thereby ensuring synchronized operation of the high voltage inverter circuitry and the low voltage inverter.

The a-c output of Q207 and Q208 is applied to step-up transformer, T101, which delivers a peak output voltage of 250 to 1000V depending on the setting of R107, the high voltage adjust potentiometer. Rectification of the output of T101 is obtained by using voltage quadrupler circuit Z401.

Regulation is obtained using the negative feedback provided by the current which flows through resistors R301, R302, and R303. This current is used to counterbalance the control current which flows through resistor R106. Any net unbalance between these two current sources is amplified by Z101 and level changer transistor Q104. The output of Q104 is used to drive the power output stage Q103. A current limit circuit consisting of Q102 and monitor resistor R103 is used to short out the output of Q104 so as to prevent excessive current flow through Q103 in the event of a malfunction in the regulator. The output of Q103 is used to provide d-c power to the center tap of the primary winding of T101. The action of amplifiers Z101, Q104, and Q103 are such that any tendency of the high voltage output to be low will result in an increase of d-c voltage at the center tap of T101. This, in turn, will result in increased a-c output from T101 and also in increased high voltage d-c output. Conversely, any tendency of the high voltage output to be high with respect to the setting of R107 will result in a decrease in the d-c voltage applied to T101 and a consequent decrease in the high voltage d-c output.

The output voltage relative to the setting of the potentiometer R107 is given by:

$$E_{HV} = \frac{\left(1 + \frac{R_f}{R_m} + \frac{R_f}{R_i}\right) E_{ref} - \frac{R_f}{R_i} E_{pot} + E_{offset} \left(1 + \frac{R_f}{R_i} + \frac{R_f}{R_{in}} + \frac{R_f}{R_m}\right)}{1 + \frac{1}{K}\left(1 + \frac{R_f}{R_i} + \frac{R_f}{R_{in}} + \frac{R_f}{R_m}\right)}$$

where R_f = (R301 + R302 + R303), R_i = R126, R_m = R112 + R113, E_{ref} = V_{CR101} = 11.7V, E_{pot} is the voltage at the arm of R107. Resistor R_{in} represents the equivalent input impedance of the operational amplifier, E_{offset} represents the input offset of the operational amplifier, and K represents the combined effect of operational amplifier gain, step up ratio of T101 and the multiplication factor (x 4) of the voltage quadrupler. Because of the high gain, low input offset, and high input impedance characteristics of the operational amplifier, the equation simplifies to:

$$E_{HV} = \left[1 + \left(\frac{1}{(R112+R113)} + \frac{1}{R126}\right)(R301+R302+R303)\right] 11.7 - \frac{(R301+R302+R303)}{R126} E_{pot}$$

A precise monitor of the high voltage output is obtained using a second operational amplifier Z102 with a level changer consisting of CR102, Q105, Q106 and associated passive components. The high voltage monitor circuitry measures the voltage drop across control resistor R106 and translates it to an output voltage which is proportionate to high voltage output. The accuracy to which the high voltage can be determined is about ± 0.2 percent and is limited primarily by the stability of the operational amplifiers and by the stability of the resistors which appear in the above equation for high voltage.

The signal processing circuitry in the high voltage module is powered in part by the regulated +23V output of the low voltage electronics unit and also by a dual isolated supply obtained by

rectifying a specially insulated output winding of transformer T201. For each of the two isolated d-c outputs an active two transistor filter is used to reduce output ripple to a negligibly low value in order to provide ripple free power to the very critical electrometer amplifier circuits. Besides the electrometer amplifier, the output voltages of the isolated supplies, nominally +16V, are used to power an electronic calibrator circuit and the two voltage controlled oscillators associated with the electrometer amplifiers.

The electronic calibrator is used during the pre-launch countdown operation to provide a 10^{-8} ampere and 3×10^{-6} ampere simulated input to the electrometer amplifiers in order to obtain a final check on system calibration. For each calibration current, a relay circuit is used to disconnect the photomultiplier output signal an and to replace it by a precise current source. The overall accuracy of the calibration current is about $\pm$ 1 percent. This is accomplished by using precision resistors and a zener diode reference circuit to obtain the calibration currents. The two calibration relays are isolated from ground and may be operating as high as 3600V above payload ground potential. Consequently, two optical isolators each having an insulation rating of 5000V are used to translate the 28V hi cal and low cal calibration command signals from the payload ground reference to the isolated common associated with the calibration relays. The output of each optical isolator is applied to the associated relay circuit using a single stage buffer amplifier to provide the drive current required to operate the relay coil.

The electrometer amplifiers consist of conventional high gain, high input impedance (FET input) operational amplifiers connected in the inverting mode. The same basic circuit is used for the linear and the logarithmic electrometers. However, in the case of the linear electrometer a 100 meg resistor is used in place of the logarithmic feedback element. The temperature compensation circuitry associated with the logarithmic element is not needed for the linear electrometer and is therefore omitted.

The feedback element is a precision resistor for the linear amplifier and a diode connected field effect transistor for the logarithmic amplifier. The logarithmic electrometer amplifier also contains temperature compensating circuitry that is used to cancel out the effects of parametric variations in the feedback diode characteristics caused by changes in ambient temperature. The temperature characteristic of a typical log electrometer is shown in graphical form in Figure 16. The response time for the logarithmic electrometer itself is determined primarily by the time constant of the feedback element. The feedback impedance can be represented by a shunt capacitance of approximately 10^{-11} farads in parallel with a resistance whose value is dependent on input current. The resistance-current relationship for the 2N5199 element which is used as a logarithmic diode is given by:

$$R_{dynamic} = \frac{T}{10719I}$$

where I is the input current in amperes and T is the temperature in degrees Kelvin. For an input current of 10^{-9} amperes and an ambient temperature of 300^{o}K the response time constant will be

$$\tau = R_{dynamic} \times C_{parallel}$$

$$\tau = \frac{300 \times 10^{-11}}{10719 \times 10^{-9}} = 280\ \mu sec$$

In terms of frequency response this would correspond to a 570 Hertz cutoff frequency. For higher values of input current the frequency response would be even better. Thus, it can be seen that for the logarithmic channels of the Chaser photometer the primary limitation of system bandwidth results from the choice of relatively low values for the subcarrier frequencies which have been used.

In the case of the linear channels the electrometer frequency response is governed by the 100 meg feedback resistance

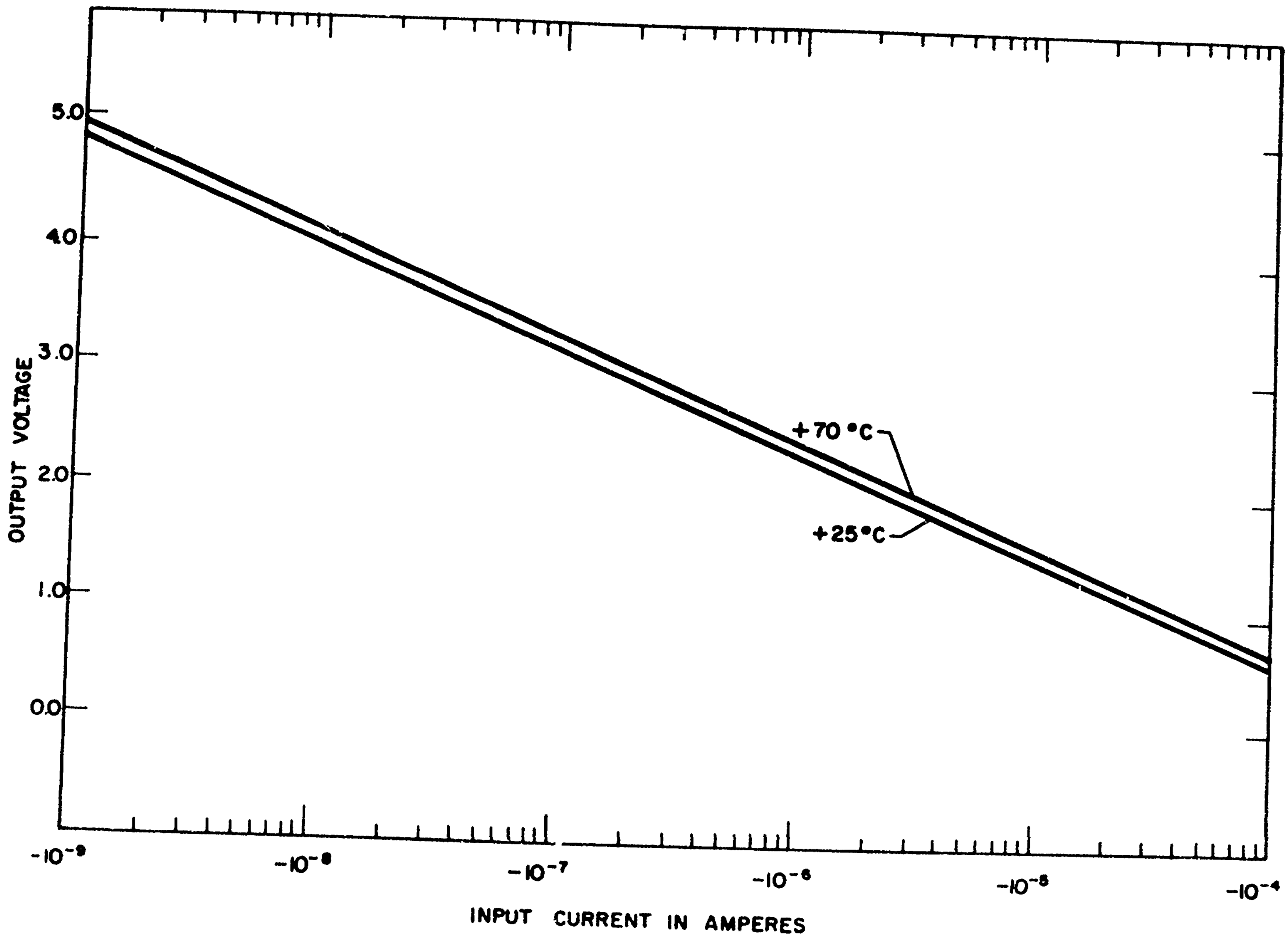

Figure 16. Temperature Characteristic of Typical Log Electrometer

element. This in parallel with an estimated 3 pf of distributed feedback capacitance results in an amplifier time constant of

$$\tau = R_f \times C_f = 10^{+8} \times 3 \times 10^{-12} = 300 \ \mu\text{sec}$$

The corresponding value of upper 3 db cutoff frequency is

$$f_c = \frac{1}{2\pi\tau} \approx 500 \text{ Hertz}$$

In addition to the internal bandwidth limitations just discussed, the output signals of the PM tube are also filtered in the 230 Hertz input filter circuit previously discussed. This input filter is common to both the linear and logarithmic channels and, in equivalent circuit form, consists of a 1.67 megohm resistor (R504 and R505 in parallel), which is in shunt with a 417 picofarad condenser (C501 in parallel with C502 and C503). The cutoff frequency associated with the input filter is therefore given by:

$$f_c = \frac{1}{2\pi \times 1.67 \times 10^6 \times 417 \times 10^{-12}} = 230 \text{ Hertz}$$

The actual module used for the logarithmic electrometers makes use of the GCA Model DP-2000A KG circuit. The same circuit, but with a 100 megohm resistor substituted for the log diode and with the temperature compensation deleted, is used for the linear amplifier. Detailed specifications for the GCA Model DP-2000A KG logarithmic electrometer amplifier are included in Appendix B.

The output of each electrometer amplifier is converted to frequency modulated form by an associated GCA Model SC-3100 voltage controlled oscillator (VCO) unit. Detailed specification for the SC-3100 VCO are presented in Appendix C.

Resistor mixing of the two VCO outputs is obtained with a trimpot, R304, in order to provide capability for changing the mixing ratio (taper) of the subcarrier output levels.

The mixed output is translated to telemetry ground using a unity turns ratio transformer designed with sufficient insulation to withstand the 3600V stress between the primary and secondary windings. The output of the transformer is processed by a variable gain buffer amplifier, Z103, consisting of a feedback connected operational amplifier. The a-c coupled output of the buffer amplifier is applied to one of the coaxial output jacks, A2, in the low voltage electronics unit. The output of A2 is delivered to the telemetry portion of the payload where it is linearly mixed together with the other VCO outputs.

When the telemetered signal is processed by a ground station discriminator, the recovered signal in each photometer channel will encounter additional low pass filtering. For the linear channels (subcarrier channels 11, 12, and 13) the normal cutoff frequencies are 110, 160 and 200 Hertz. However, for the early flights in the Chaser program, an 11 Hertz post detection filter was used to condition the outputs of the linear channels in order to reject the 60 Hertz interference which originates the motor supply circuit.

For the logarithmic channels the usual cutoff frequencies are 45, 59, and 81 Hertz for subcarrier channels 8, 9, and 10. Because these cutoff frequencies are considerable lower than the photometer cutoff frequencies, care should be taken to properly interpret the output signals for the log channels particularly if large high frequency fluctuations are found to be present in the signals. Fortunately, the sensitivity of the logarithmic channels is low enough that interference effects from the motor supply circuit can be ignored. Consequently, additional post detection filtering is not required for the signals in the logarithmic channels.

IV. DAYTIME MODIFICATION; BAFFLE PLATE SYSTEM

The basic photometer payload package has been described in detail. It is emphasized that for the intitial exploratory experiments it was propitious to achieve maximum throughput for optimum signal detectivity so that only nominal baffling could be applied.

Owing to the nature of the data acquired on the initial Chaser nighttime experiments, it was decided to modify the basic payload photometers so that field operations during daytime hours could be accommodated. The major modification requirement involved the ability to efficiently baffle out strong stray radiation present for experiments performed under solar illuminated conditions. For this purpose, an appropriate baffle system was designed, fabricated, installed, and tested for direct application to the daytime Chaser photometer configuration. The final design represented a tradeoff between stray light rejection and throughput. This design incorporated thirty-one baffles positioned as shown in Figure 17. System testing has demonstrated that the required baffling was achieved while retaining about 30 to 40 percent of the maximum nighttime sensitivity. System flexibility was realized since the daytime baffle system could be assembled or dismantled as necessitated by field program requirements.

Typical baffle spacers are shown in Figure 17 as well as the thirty-one baffle plates employed.

The assembled daytime modification was subjected to field-of-view tests to ascertain the off axis rejection factors as a function of viewing angle. The tests were performed in the visible region of the spectrum since it is convenient and it also establishes conservative upper limit values since the reflectivity of the baffling surfaces is consdierably less in the VUV region than in the visible. Accordingly, a quartz iodide source provided sufficient intensity output to perform the measurements throughout the dynamic range required. The lamp radiation was collimated with a large aperature lens to fully illuminate the photometer entrance aperature. The data were collected by recording the output as a function of rotation angle about an axis normal to

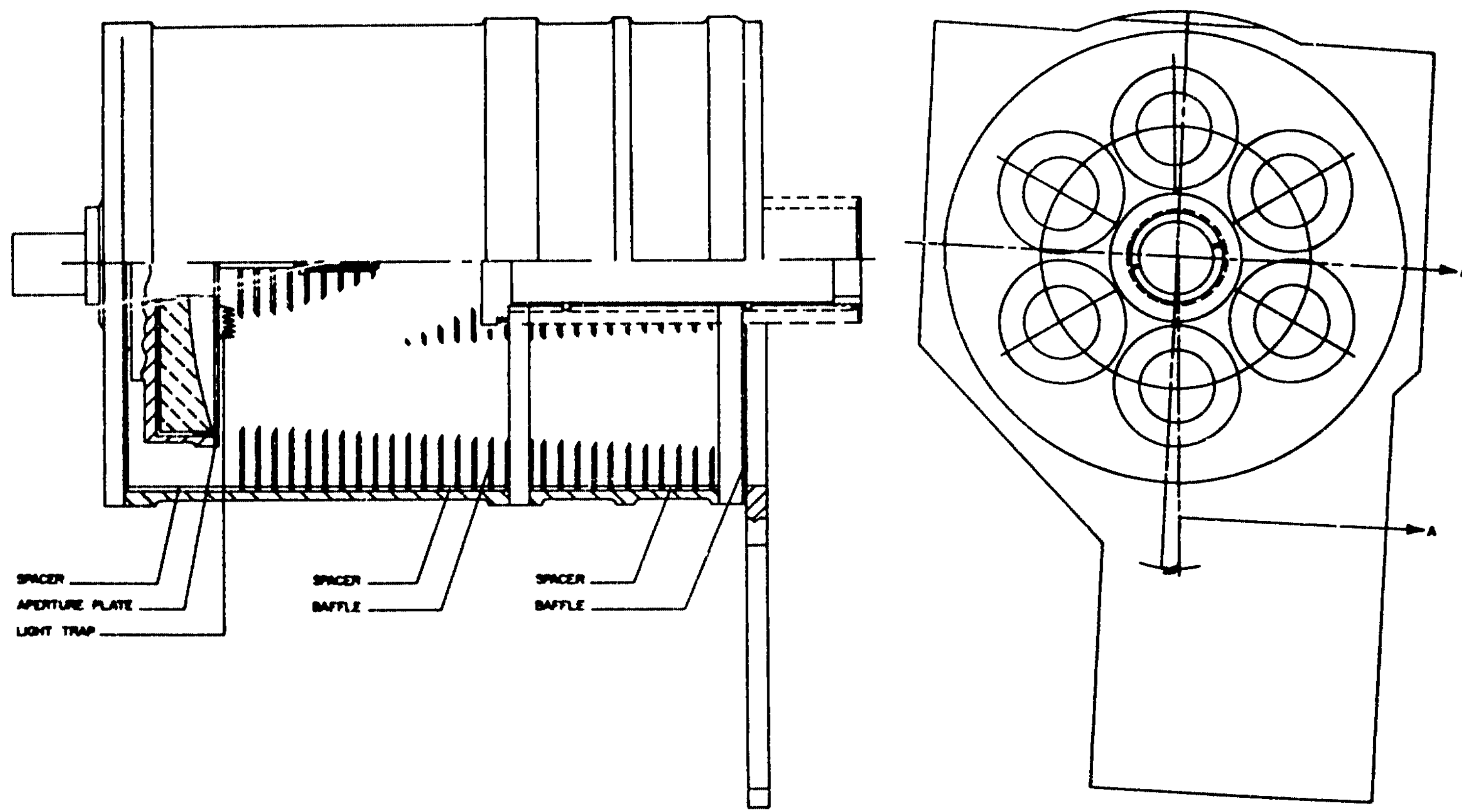

Figure 17. CHASER Daytime Modification

the optical axis which was situated in the plane of the entrance aperature.

Owing to the large dynamic range involved, it was necessary to collect the data in several angular increments. In each case, care was exercised to assure that each adjacent angular increment provided sufficient overlap to normalize the output in each successive case.

The curve shown in Figure 18 represents a composite of the data acquired by the normalization procedure described. The error bar shown applies at about $\pm$ 30 degrees and represents a cumulative error which increases on a relative basis as the angle increases. The derivation of this error estimate is not included herein but it was obtained using the weighting factors involved in the several individual curves employed. In any case, the data shown in Figure 18 demonstrates the high degree of rejection achieved; these data can be applied to feasibility analyses on proposed Chaser experimental configurations.

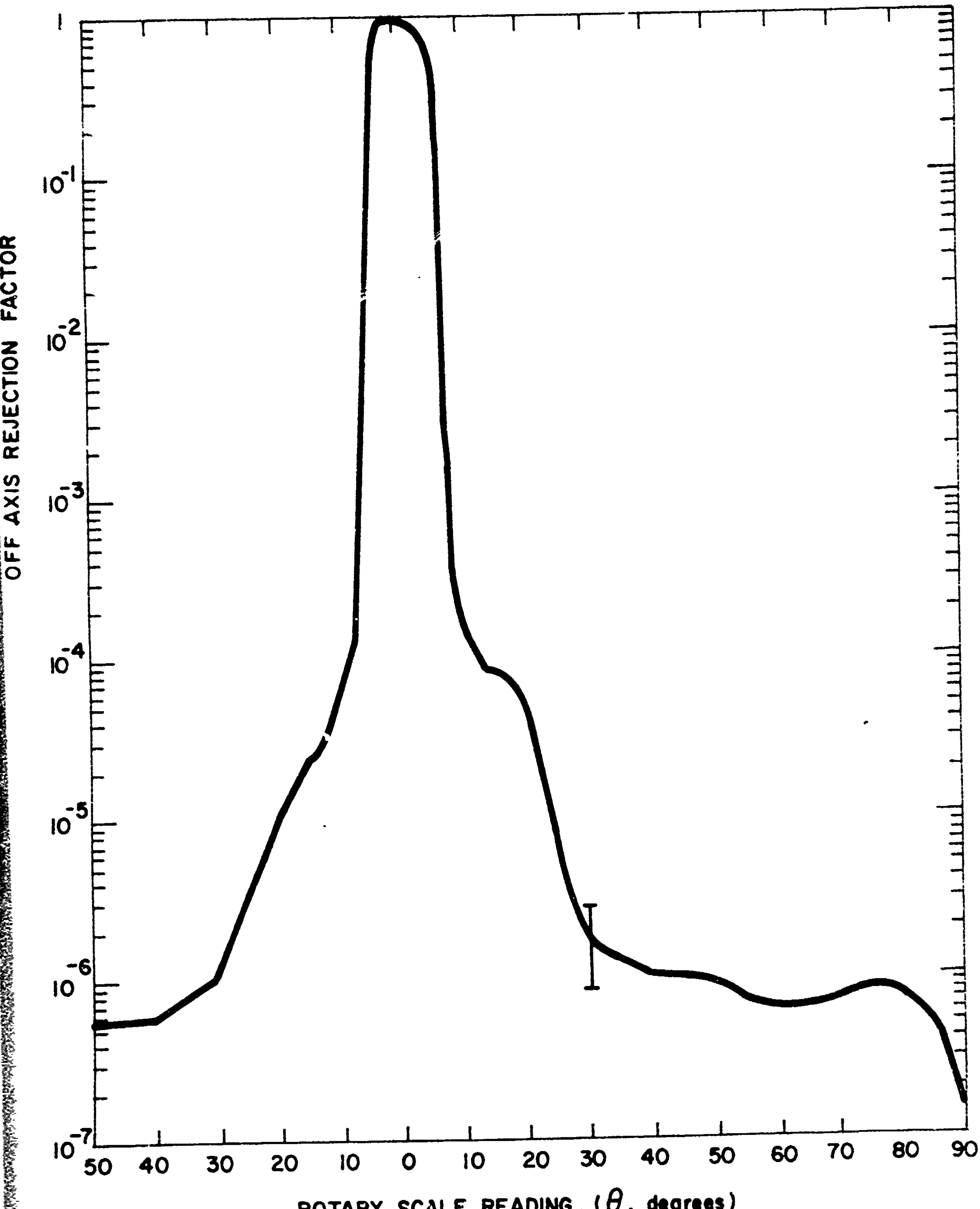

Figure 18. Daytime Modification System Off Axis Rejection Factor as a Function of Rotary Scale Reading, in Degrees

V. BELT SCANNER SYSTEM

The data acquired during the initial CHASER field experiments yielded quantitative signal intensity information as well as upper limit values for signal spatial characteristics. However, owing to system requirements it was considered useful to modify the basic photometer to achieve more definitive data on the detected target spatial characteristics, i.e., size, shape, intensity distribution, etc. For this purpose, it was demonstrated that this could be accomplished most easily and efficiently by insertion of an appropriately designed belt scanner system in the focal plane of the photometer just prior to the PM tube detector system. The salient features of the belt scanner system can be best illustrated with initial reference of Figures 19, 20, and 21.

Figure 19 shows a schematic presentation of the assembled belt scanner system; Figure 20 shows the assembled belt scanner with the motor and sensor electronics attached. In this format it is a simple matter to visualize the assembled modified photometer package, including the scanner belt positioned in the focal plane. Figure 21 shows the disassembled belt scanner system. The major component on the system is the scanner belt itself. It was designed to perform a continuous scan of the entire field of view within increments of less than one degree over an adjustable time period of between one to five seconds. The remainder of the system components were employed to both perform this function as well as to sense and record the sequence of signals acquired during flight.

However, a number of specific important tasks, modifications and tests were performed before successful operation was achieved and verified in the field as discussed below.

First, it was of prime importance to properly position the 0.001" stainless steel scanner belt in the "focal" plane with regard to an identifiable reference plane, which for this task, was the end of the photomultiplier housing structure which is suspended concentrically

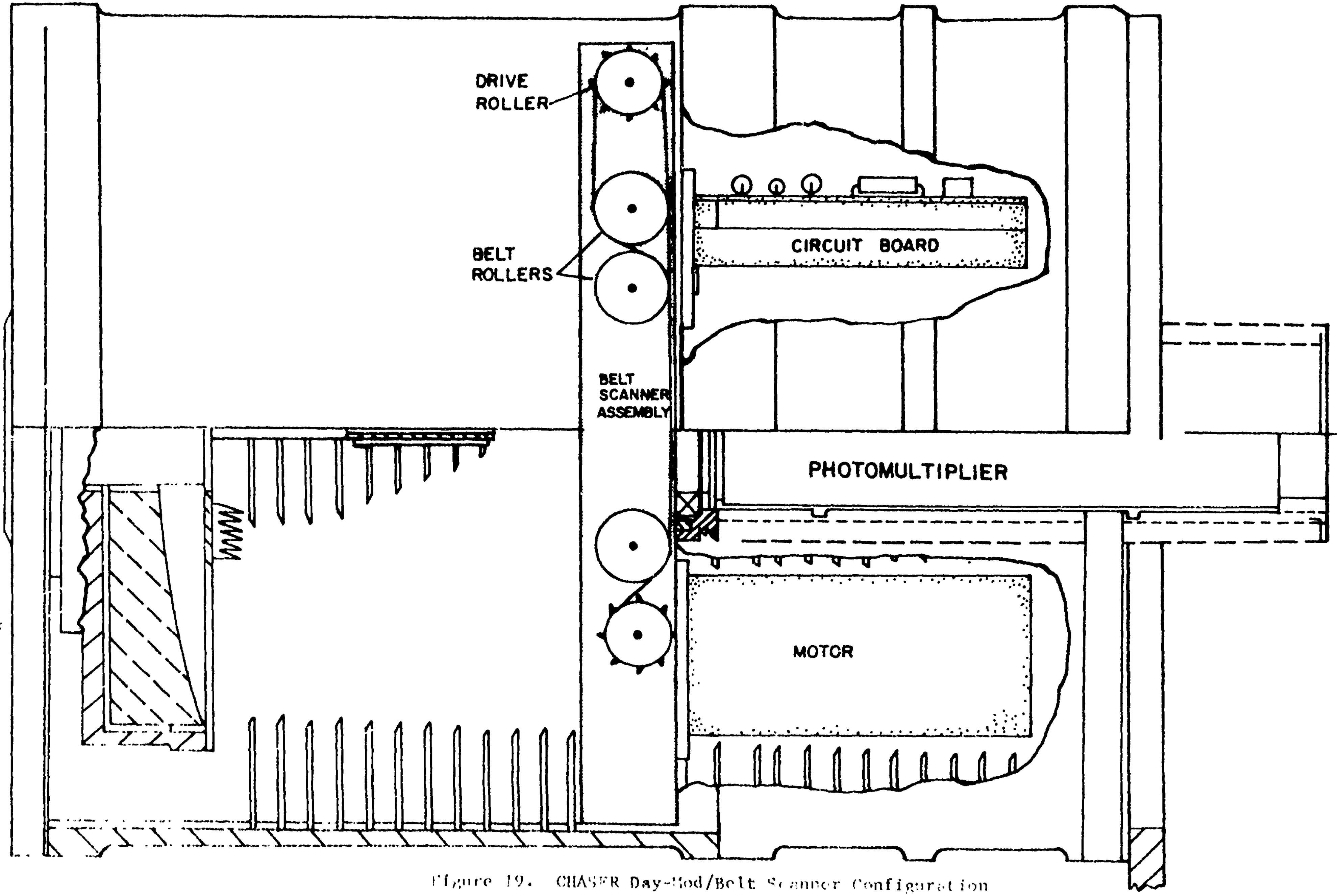

Figure 19. CHASER Day-Mod/Belt Scanner Configuration

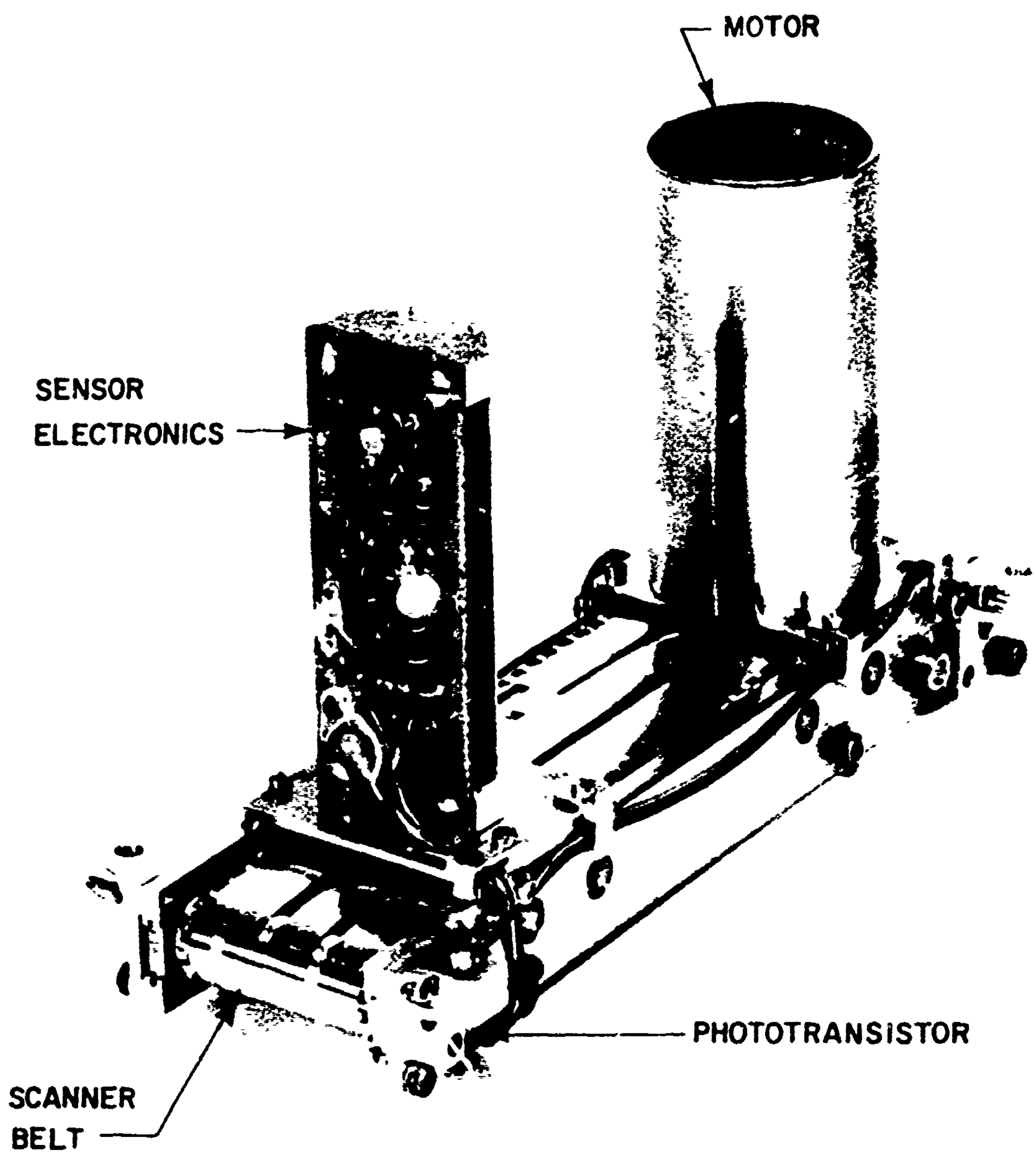

ASSEMBLED BELT SCANNER

Figure 20 Photograph of assembled belt scanner module with sensor electronics and motor attached.

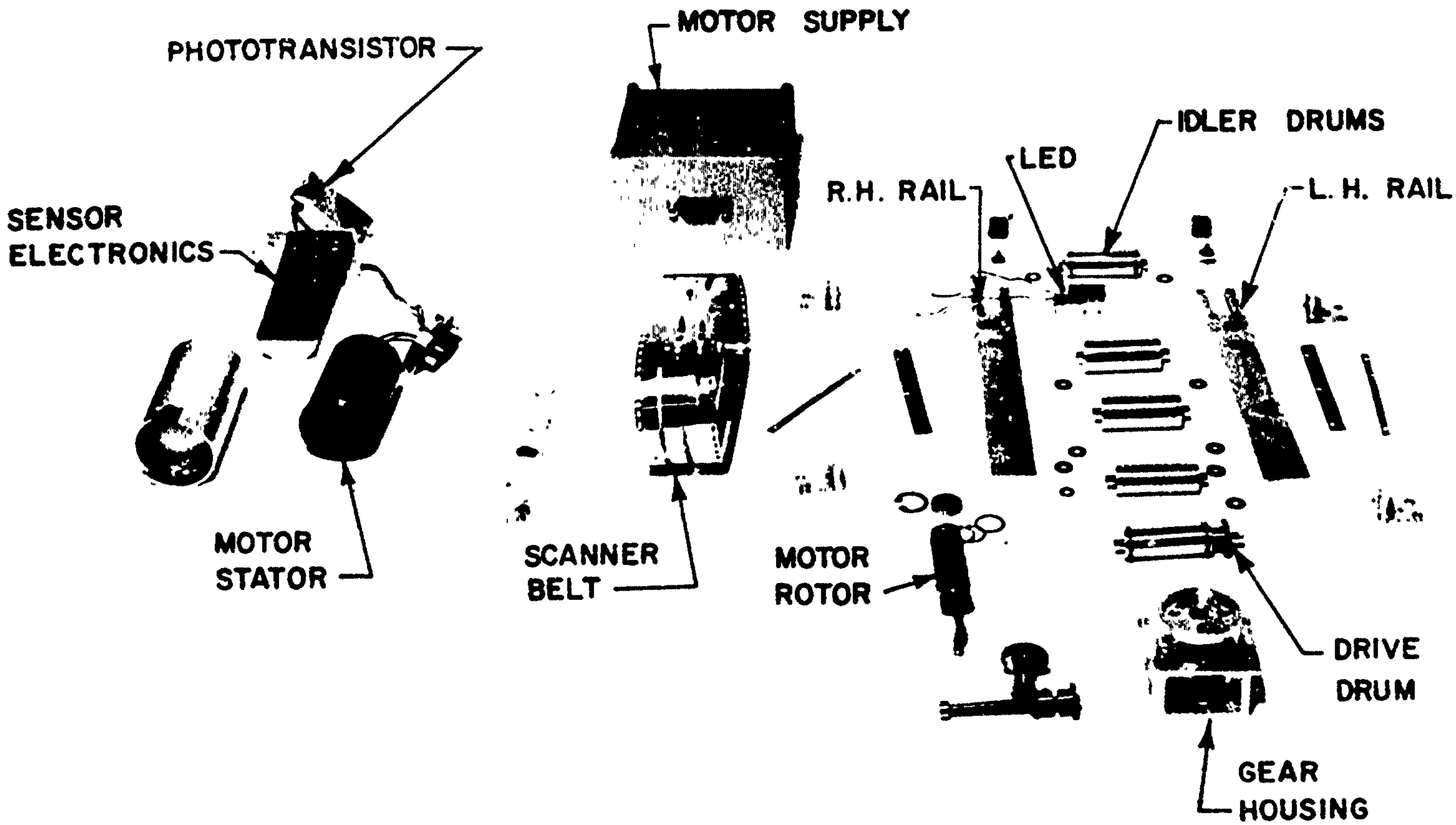

Figure 21 DISASSEMBLED BELT SCANNER SYSTEM

within the cylindrical photomultiplier housing. The procedure adopted can be conveniently discussed with initial reference to the data shown in Figure 22 which indicates a point source effective diameter as a function of positions along the optical axis of the photometer (solid curve) as well as along the edge of the field of view (dotted curve). With the aid of the data shown in the Figure it then became possible to determine the best compromise position of the belt scanner belt. It turns out that the required adjustment could be achieved by moving the mirror backward to accommodate and properly position the belt. In the basic unmodified instrument the focal plane was necessarily positioned inside the PM housing structure. In the present case, the scanning foil could not physically penetrate inside the housing structure, an alternate approach was devised. The approach adopted was to cut off the main mirror mounting ball structure (which was originally designed to permit the mirror to be properly aligned). Thus, a trade-off was established whereby this necessary feature was incorporated at some sacrifice of mirror alignment (which incidentally is not as essential for the scanning system, as it is in the case of, say, the rotating reticle system).

The actual image spot was not a clean circle but rather a six point star-shaped illuminated pattern that was not uniform. Additionally, its shape and illumination varied with axial position. The curves shown in Figure 22 represent the diameter of a circle within which the star can be inscribed. The dashed curve represents the diameter for the edge of the field of view, whereas the solid curve is the same for the axial location. As may be seen from the Figure, the definition of the "focal" plane is a somewhat arbitrary matter; in this case, the original focal plane was moved back about 3.25 mm as a compromise value. The measurements were performed with the use of a light bulb at the distance of 100 feet. The diameter of the light source was in all cases less than the projected diameter of the spot size in object space so that for all practical purposes the light bulb could be considered a "point" source. Finally, since the source used in this case was not at infinity but at the above noted 100 feet, a correction

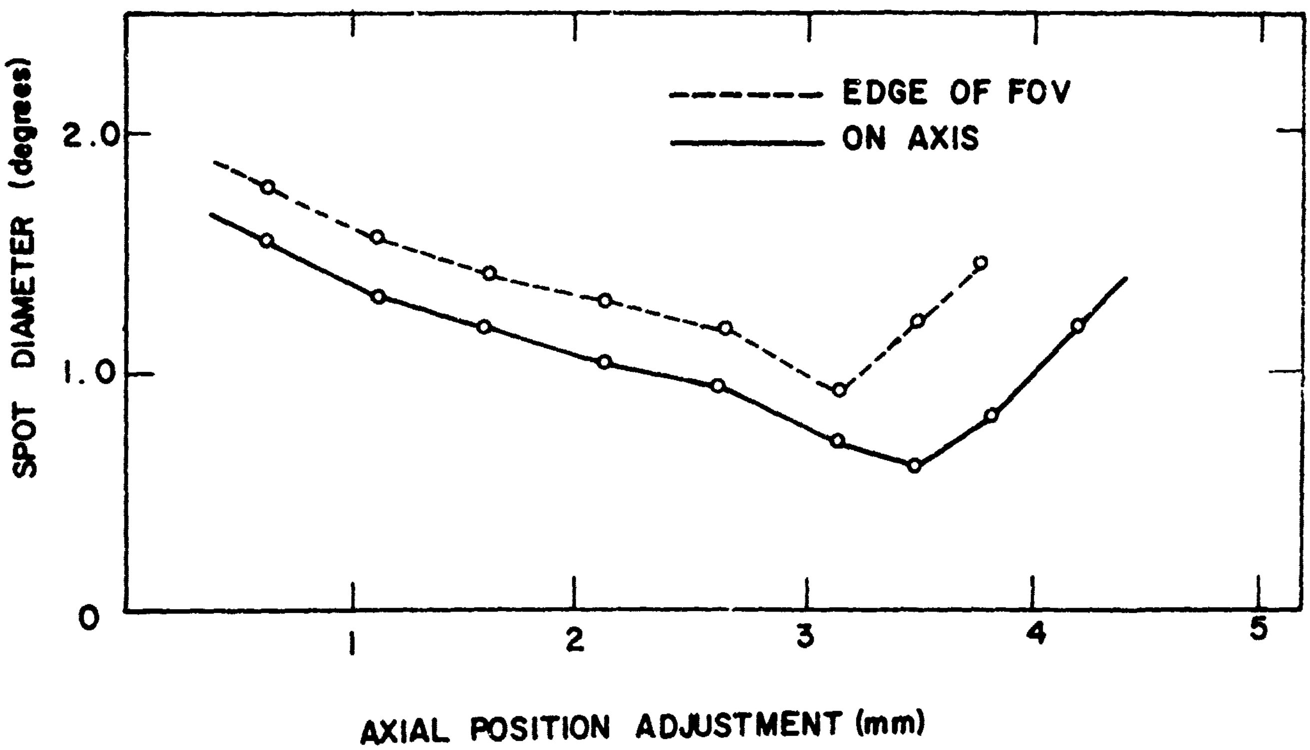

Figure 22 Point source apparent spot diameter vs. mirror axial adjustment position. 'he dotted curve obtains for edge of field of view measurements whereas the solid curve obtains for on axis measurements. !hese data indicate the best compromise position for repositioning of the mirror. 'n this case the value of 3.25 mm was selected.

had to be applied to the axial position for the equivalent location of a point source at infinity. This correction has been included in the data shown on the diagram.

The Belt Scanner System Modification involved the design, fabrication and testing of the electronic circuits required for the Belt Scanner Motor and Sensor systems. The schematic circuit for the belt scanner motor is shown in Figure 23. It may be noted that the indicated circuit follows the basic design which was normally included in the low voltage power supply units of the regular circuits as illustrated in Figure 13. However, for the present task it was found that the original location of the motor drive circuit introduced a substantial amount of 60 hertz interference into the photometer signal channels, so that a separate power module located more remotely was employed to drive the motor used in the belt scanner mechanism. The resultant effects had previously been minimized by the use of a low pass filter having a cross over frequency of 11 hertz but this would not have been possible to employ in the case of the belt scanner which had to have a response in the millisecond region.

The belt sensor circuit shown in Figure 24 illustrates the position detecting circuitry for the belt scanner. Eleven equally spaced reference holes located near one edge of the scanner belt together with a photo transistor and LED light source are used to generate the fiducial signal which corresponds to the start point of each scan. A twelfth hole equally spaced between two adjacent holes is used to establish a frame reference marker.

The belt sensor circuit is driven by a 5V regulated source which is derived from the +28V system battery using R7 and VR1. The light source for the belt sensor system is an infrared light emitting diode, CR1, which is supplied with a drive current of 20 ma (nominally) by resistor R6.

The light emitting diode is positioned such that, in the absence of the belt, it would directly illuminate the phototransistor sensor

A

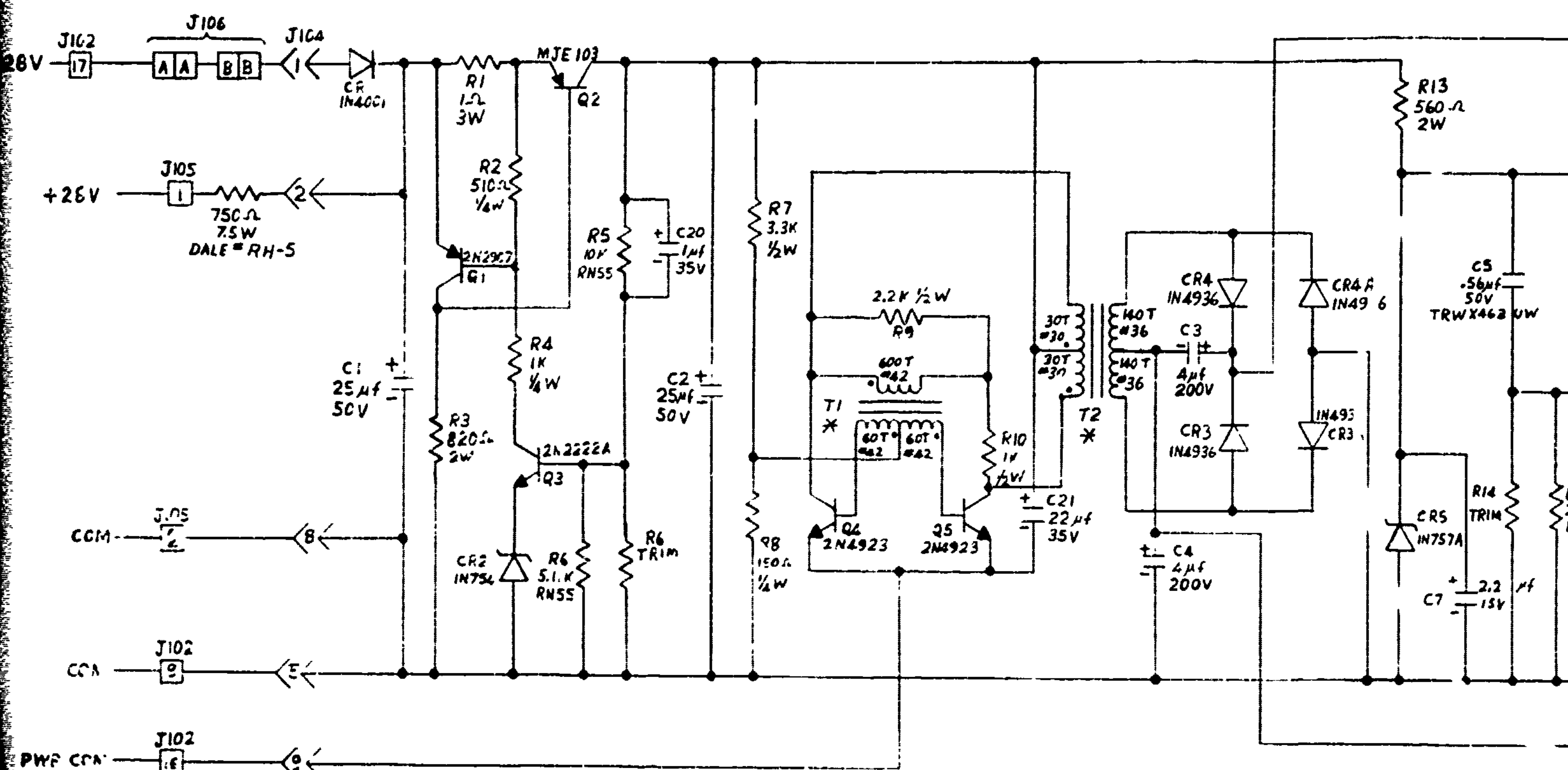

* T1 CORE – ARNOLD ENG. # 15566-P25C-53
T2 CORE – FERROXCUBE # 2213-387

Figure 23. Schematic Circuit for Belt Scan

B

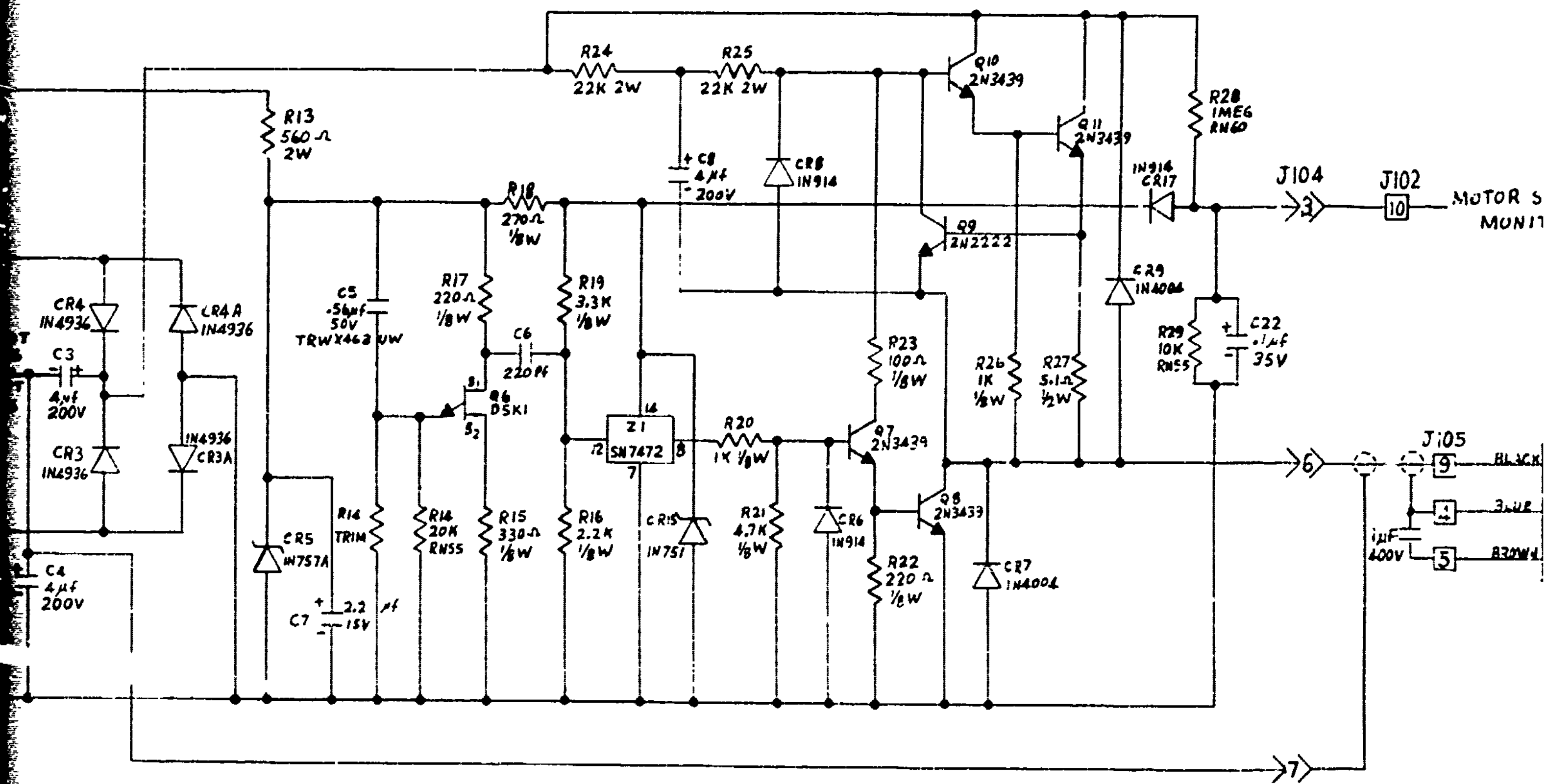

ematic Circuit for Belt Scanner Motor

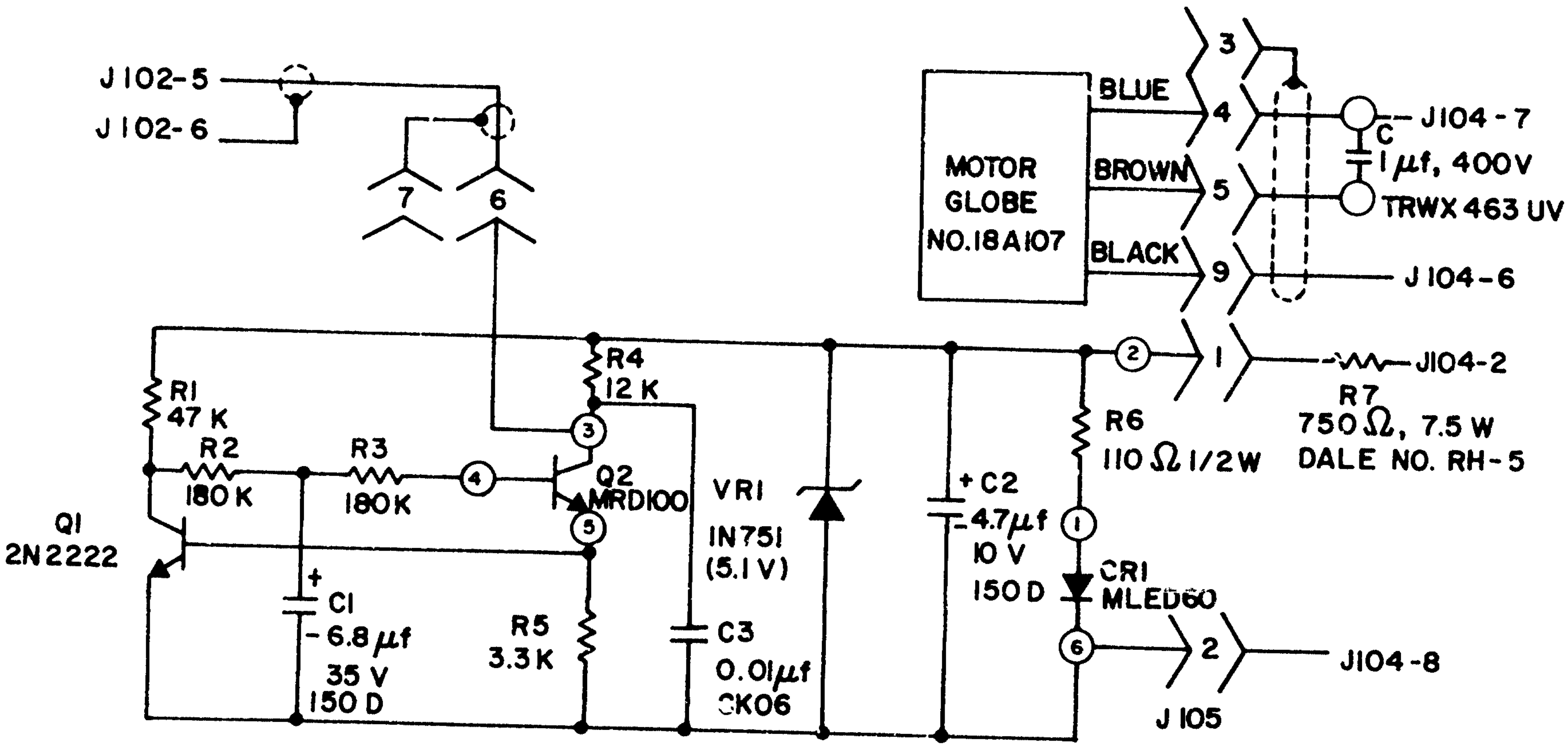

BELT SENSOR

Figure 24. Belt Sensor Circuit

Q2. However, with the belt installed, the output of CR1 is masked by the belt except for the times during which the "B" cutout shown in Figure 25 is passing between the light source and the phototransistor. In the absence of any illumination phototransistor, Q2, will be operating as a normal transistor and the voltage feedback from Q1 will serve to stabilize the transmitter output of Q2 at the + 0.6V (nominal) base to emitter threshold voltage of Q1.

The quiescent output at the collector of Q2 is therefore given by

$$5V - \frac{0.6V}{3300} \times 12{,}000 = +2.8 \text{ Volts}$$

Thus the collector output of Q2 is approximately centered with respect to the standard telemetry range of 0 to +5V. Whenever one of the "B" cutouts of the scanner belt passes between the light emitting diode and the phototransistor, Q2, the light signal will be amplified by Q2 and appear as a negative going pulse having a nominal amplitude of 2 volts.

The design constants of R2, R3, and C1 are such that the feedback time constant is long compared to the duration of the output reference pulses so that the sensor amplifier Q1, Q2 and associated components will operate with full sensitivity for pulse inputs and with low sensitivity for quiescent inputs. Consequently, in the event that some ambient light has entered into the photometer, d-c feedback from Q1 will tend to stabilize the d-c output of Q2 at a d-c voltage nominally in the range of +1.5V to +2.8V.

For conditions in which the ambient light is not sufficiently large to cause the d-c output of Q2 to be below a value of about the +1.5V level, phototransistor Q2 will continue to respond properly to the light pulses which are generated by the action of the moving "B" cutouts together with the light output of CR1.

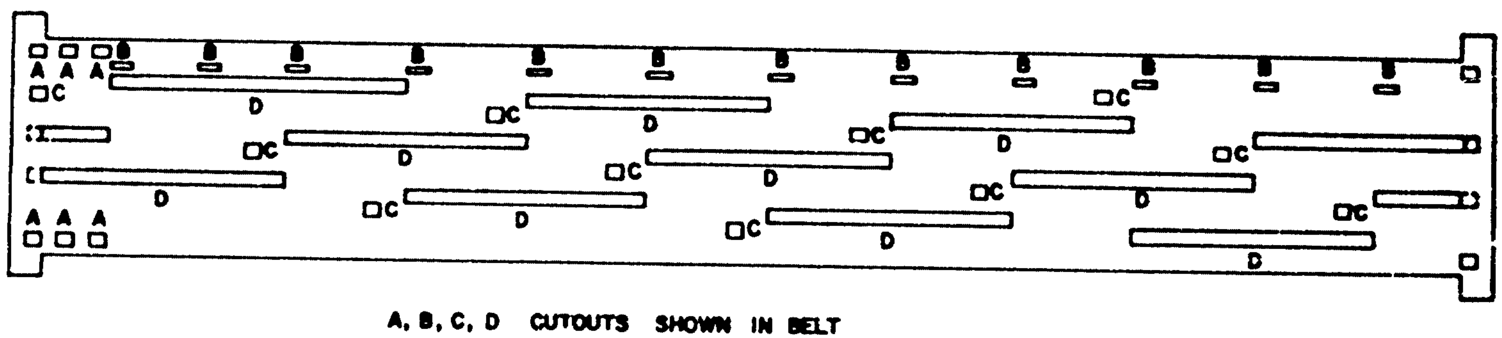

Figure 25. Schematic of Belt Scanner Employed in Daytime Modification

The assembled belt Scanner System is shown in Figure 20. The final task requirement involved testing at both the GCA and AFCRL facilities as described below.

The GCA testing procedure was limited to assuring proper mechanical operation of the device as well as the associated electronics. In addition, a number of endurance tests were performed and in all cases the instrumentation was found to operate according to within acceptable tolerances. Subsequent to these tests, the Belt Scanner Elements were installed into the Daytime Modification Photometers as illustrated in Figure 17. Daytime Photometer incorporating the Belt Scanner was then delivered to AFCRL where it was exposed to additional tests. The belt and drive mechanism was removed from the unit, and the high voltage box leak rate, and high voltage tests were performed. A calibration of absolute sensitivity vs. wavelength was achieved by illuminating a spot on the photometer mirror with a monochromatic beam of known intensity and recording the detector output. Twenty wavelengths were used throughout the region of interest. The light was focused to a spot in the center of the detector cathode with belt removed for this calibration. The next test in the sequence involved an operational check of the entire assembled photometer in a vacuum of 1×10^{-5} Torr. Results of the 30 minute run indicated a motor temperature increase of $8^{o}C$ and motor power supply temperature increase of $20^{o}C$. The test photometer was then mounted on a fixture attached to a two meter optical bench of the CRL vacuum field of view measurement system. This system illuminates the entire photometer aperature with parallel rays from an 8 inch diameter concave mirror with a monochromatic, point light source at its 165 cm focus. The photometer positioning fixture can be controlled from outside the vacuum chamber so that changes of $\pm$ 9 degrees in azimuth and elevation from the collimated light beam can be accomodated. The photometer was then positioned through a predetermined group of 37 azimuth and elevation settings within the field of view. For each individual setting the detector response from the belt scanning device was recorded on magnetic tape and displayed on an optical write

recorder. These data provided a relative sensitivity calibration over the field of view which was normalized to the absolute calibration previously performed at the center of the detector. Also detector output pulses were analyzed for position and size of the simulated point source at infinity. It is of interest to note that this test required 45 minutes of belt operating time. The belt was operated an additional 29 minutes during payload integration and environmental testing. Photometer 2B accumulated a total belt time of 204 minutes which incorporated a dress launch rehersal, two countdowns and a successful rocket flight.

On this basis, the photometer 2B was assembled and installed into the field payload for field operation for the October 1972 target opportunity. Finally, the entire GCA photometers operated in the CHASER rocket payload operated successfully in the October 1972 field program, thereby completing the task requirements of the program.

APPENDIX A

FIELD OF VIEW MEASUREMENT RESULTS

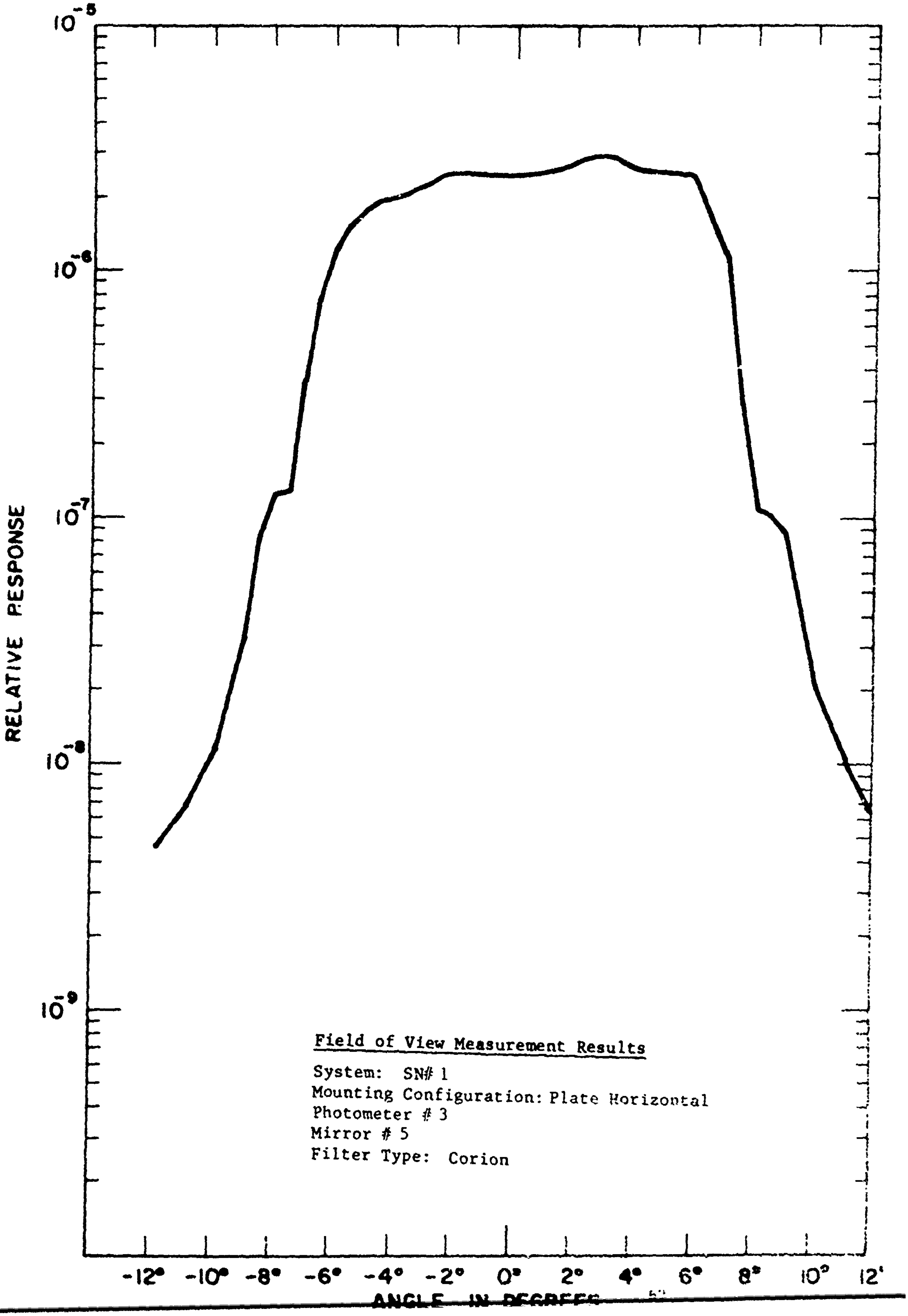
RELATIVE RESPONSE
10^{-5}
10^{-6}
10^{-7}
10^{-8}
10^{-9}
-12° -10° -8° -6° -4° -2° 0° 2° 4° 6° 8° 10° 12°
ANGLE IN DEGREES
Field of View Measurement Results
System: SN# 1
Mounting Configuration: Plate Horizontal
Photometer # 3
Mirror # 5
Filter Type: Corion

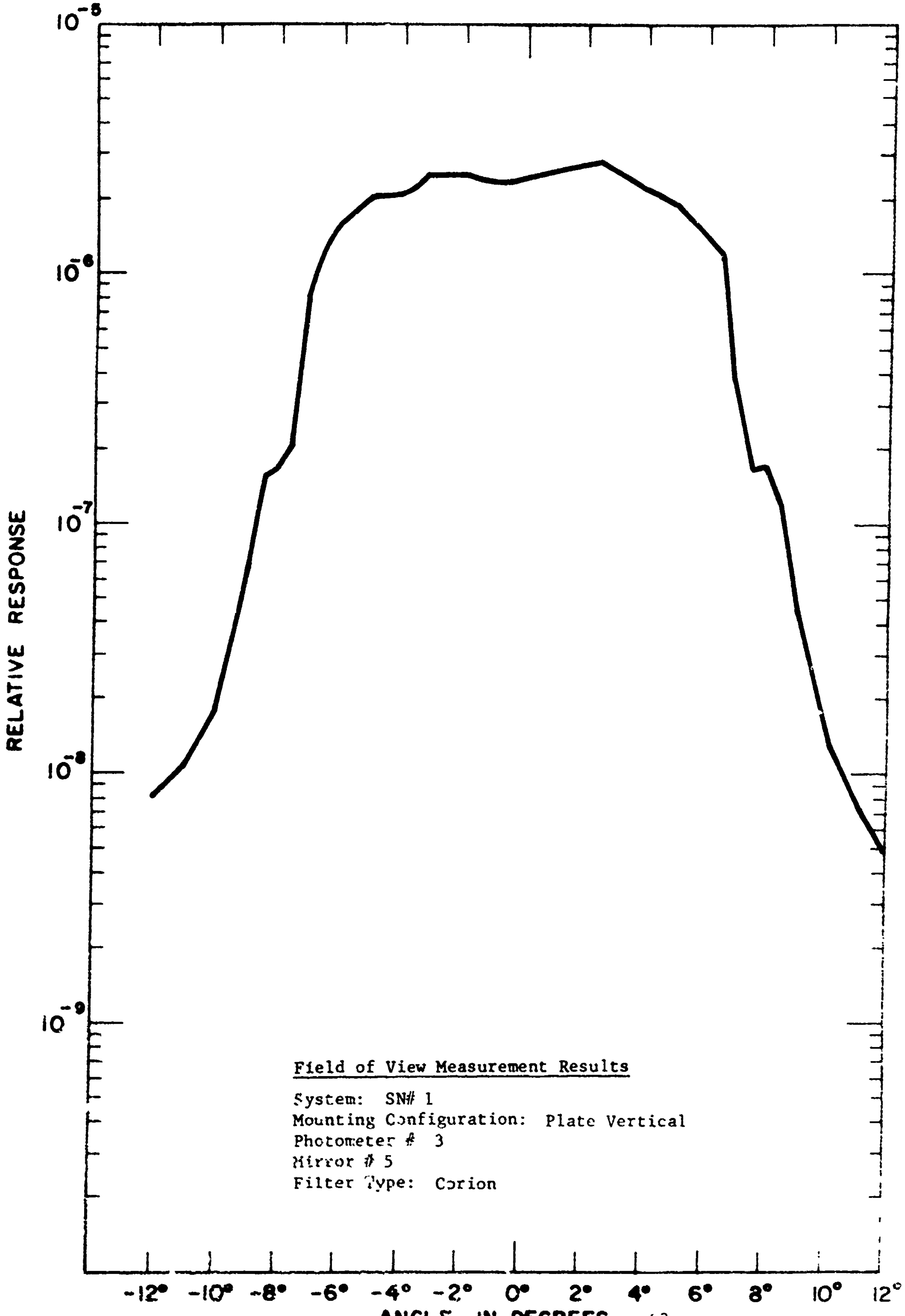
RELATIVE RESPONSE
10^{-6}
10^{-7}
10^{-8}
10^{-9}
Field of View Measurement Results
System: SN# 1
Mounting Configuration: Plate Vertical
Photometer # 3
Mirror # 5
Filter Type: Corion
-12° -10° -8° -6° -4° -2° 0° 2° 4° 6° 8° 10° 12°
ANGLE IN DEGREES

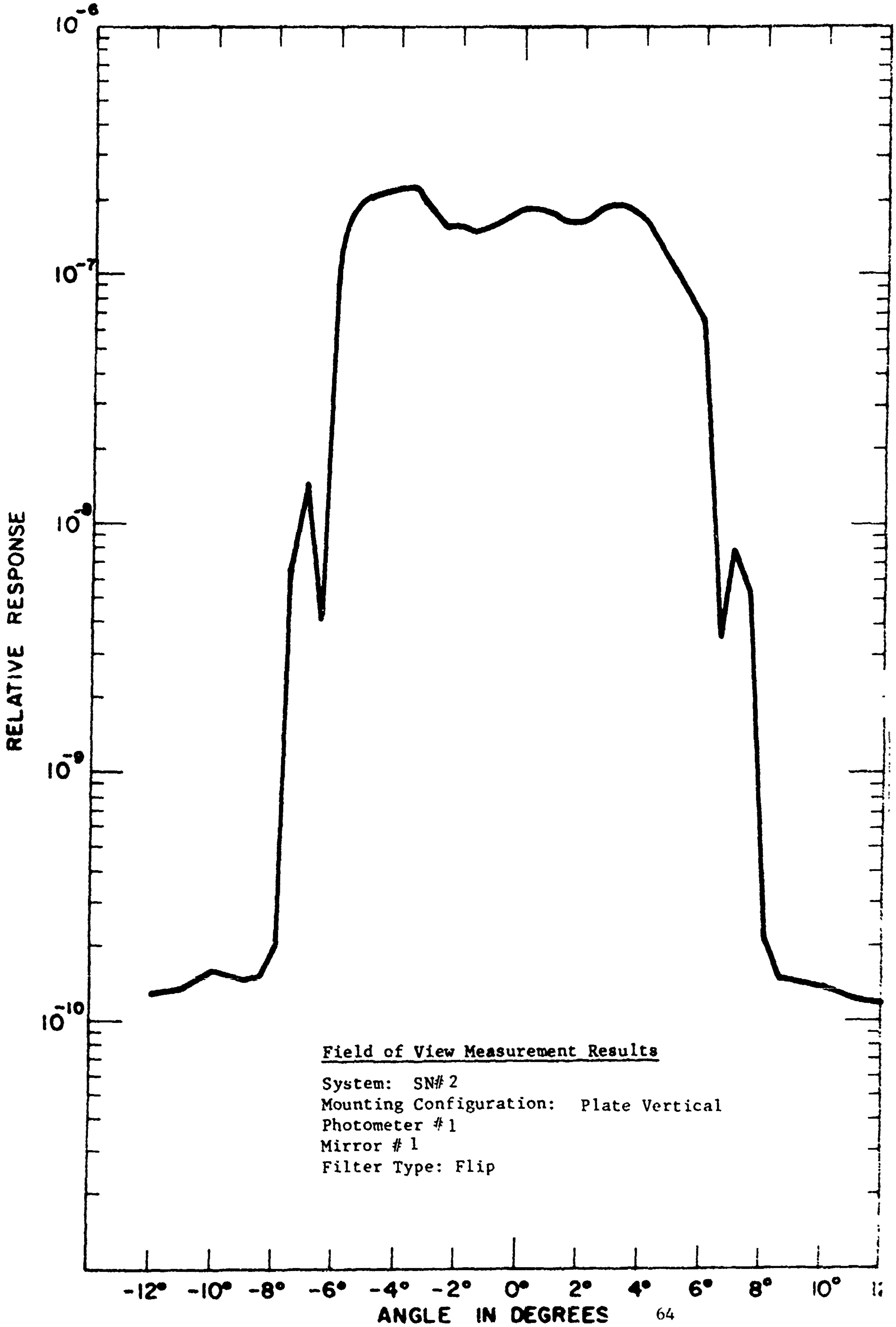

10^{-6}
10^{-7}
10^{-8}
10^{-9}
10^{-10}
RELATIVE RESPONSE
Field of View Measurement Results
System: SN# 2
Mounting Configuration: Plate Vertical
Photometer # 1
Mirror # 1
Filter Type: Flip
-12° -10° -8° -6° -4° -2° 0° 2° 4° 6° 8° 10°
ANGLE IN DEGREES

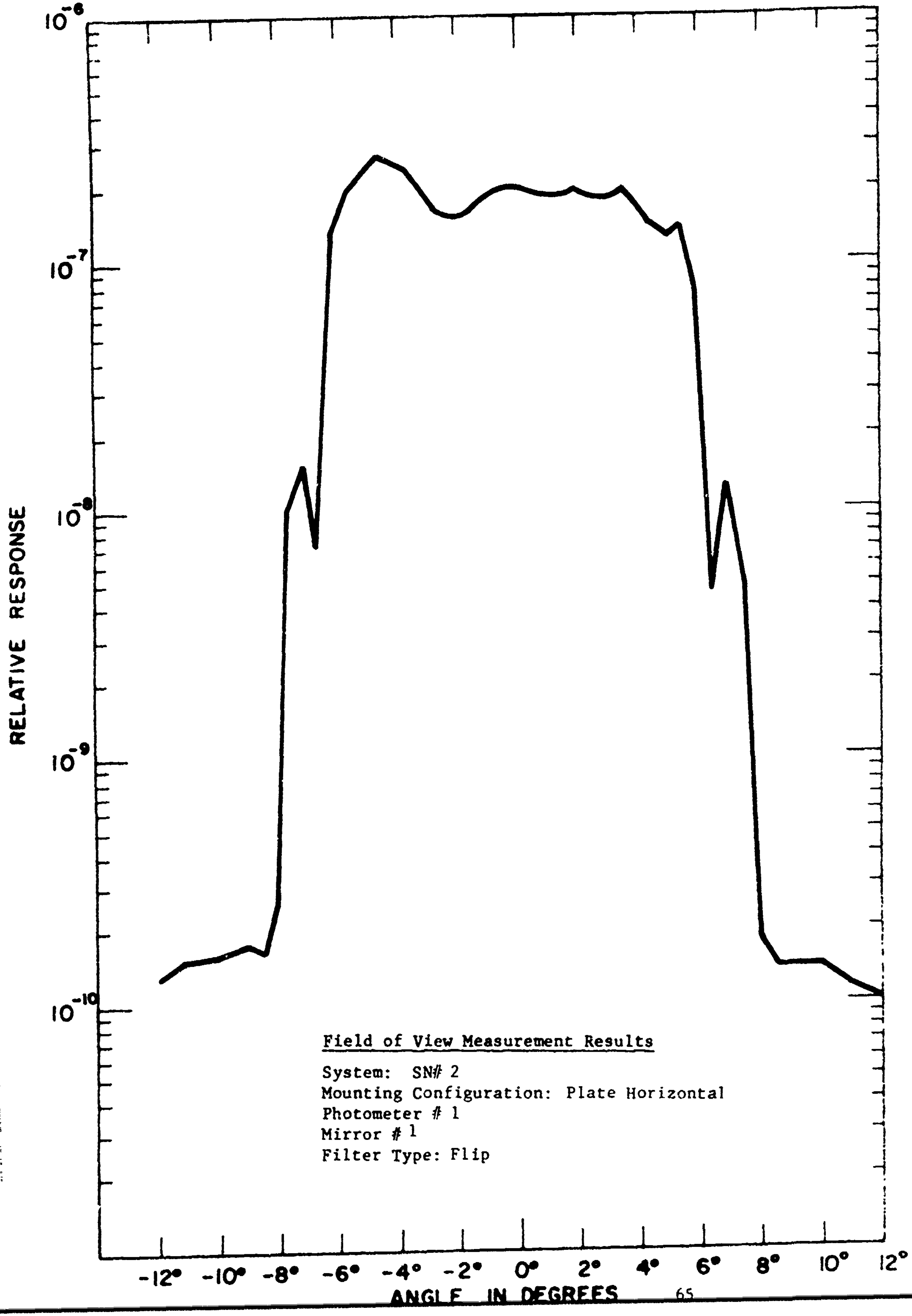
10^-6
10^-7
10^-8
10^-9
10^-10
RELATIVE RESPONSE
-12° -10° -8° -6° -4° -2° 0° 2° 4° 6° 8° 10° 12°
ANGLE IN DEGREES
Field of View Measurement Results
System: SN# 2
Mounting Configuration: Plate Horizontal
Photometer # 1
Mirror # 1
Filter Type: Flip

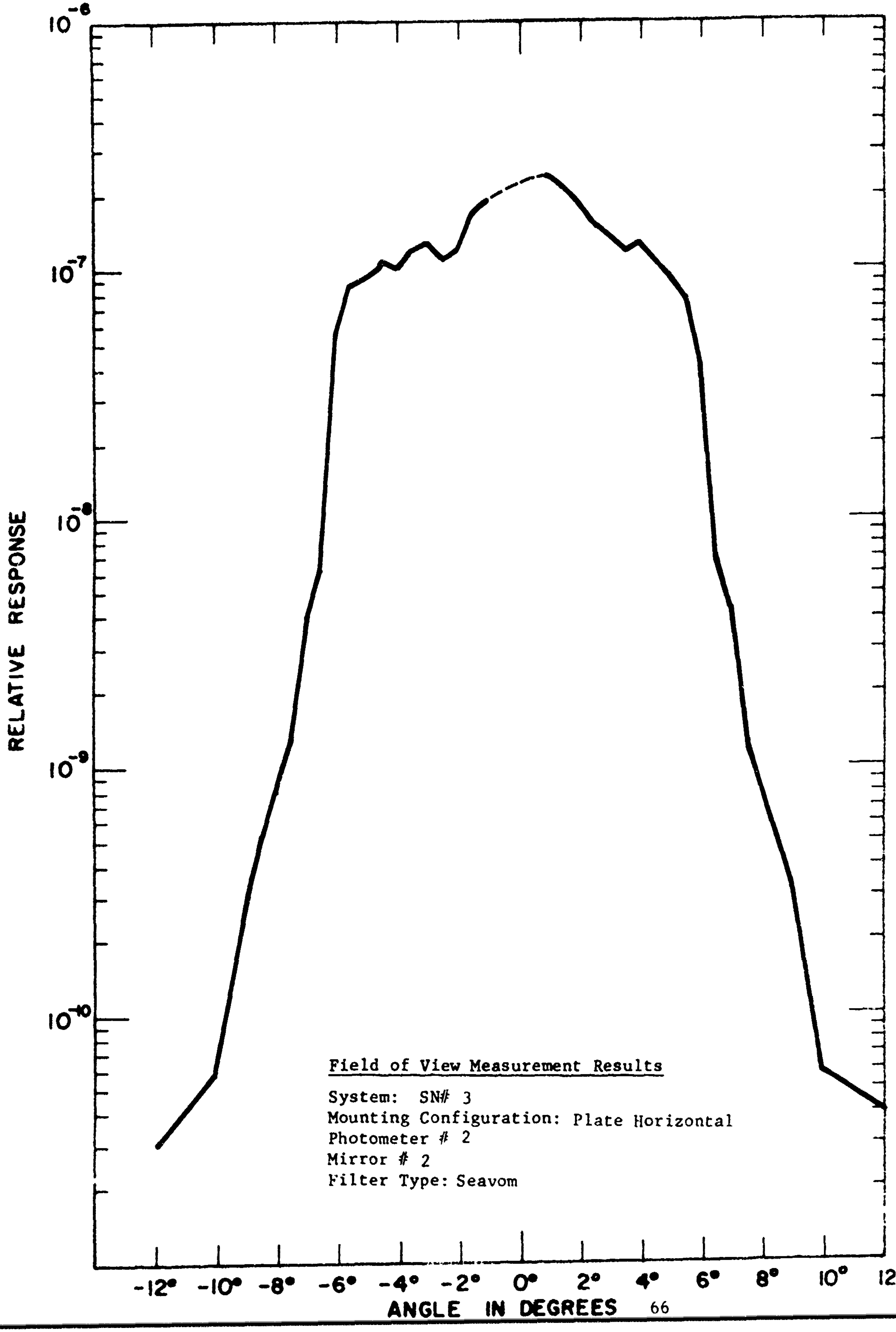
10^{-6}
10^{-7}
10^{-8}
10^{-9}
10^{-10}
RELATIVE RESPONSE
-12° -10° -8° -6° -4° -2° 0° 2° 4° 6° 8° 10° 12
ANGLE IN DEGREES
Field of View Measurement Results
System: SN# 3
Mounting Configuration: Plate Horizontal
Photometer # 2
Mirror # 2
Filter Type: Seavom

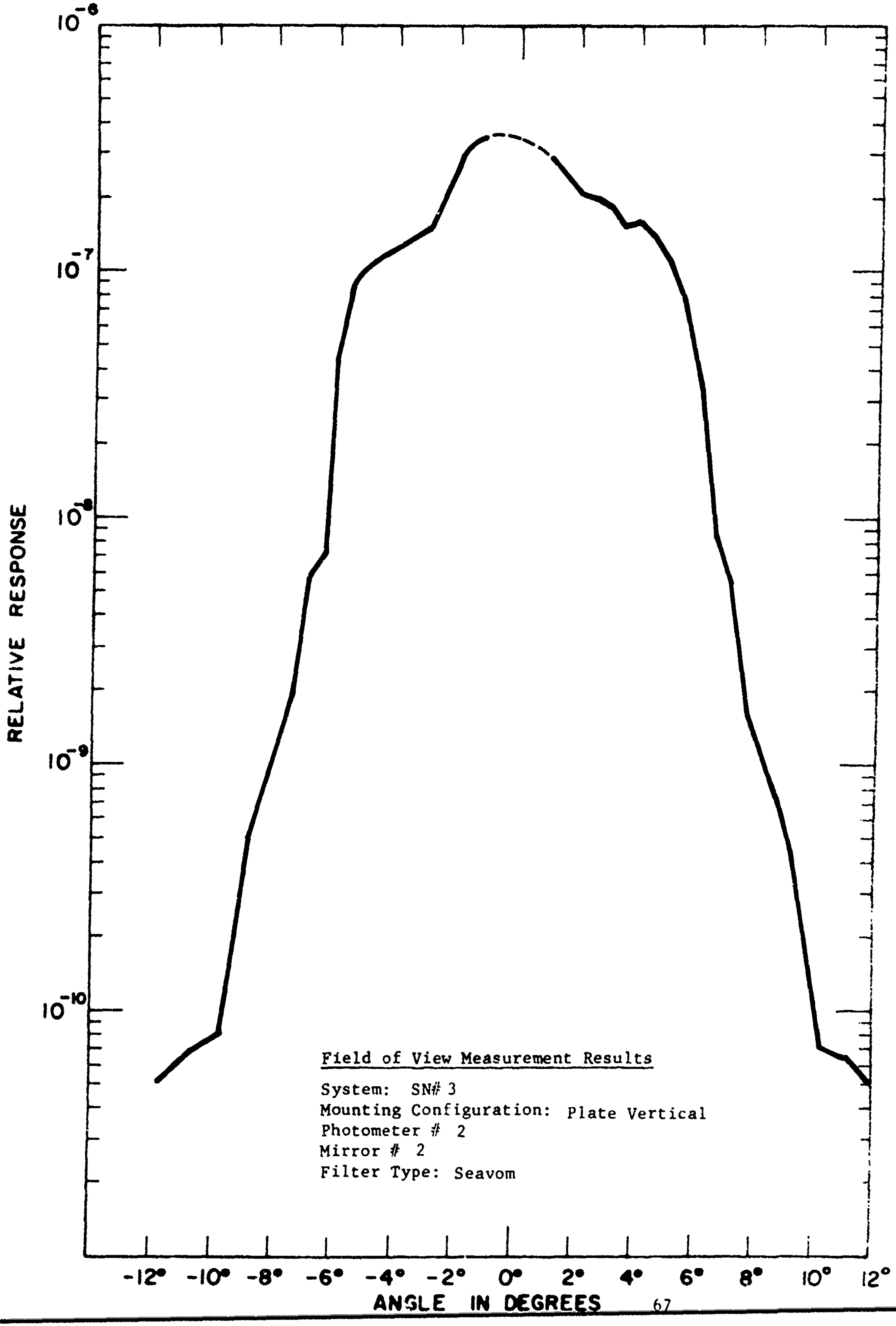

10^{-6}
10^{-7}
10^{-8}
10^{-9}
10^{-10}
RELATIVE RESPONSE
-12° -10° -8° -6° -4° -2° 0° 2° 4° 6° 8° 10° 12°
ANGLE IN DEGREES
Field of View Measurement Results
System: SN# 3
Mounting Configuration: Plate Vertical
Photometer # 2
Mirror # 2
Filter Type: Seavom

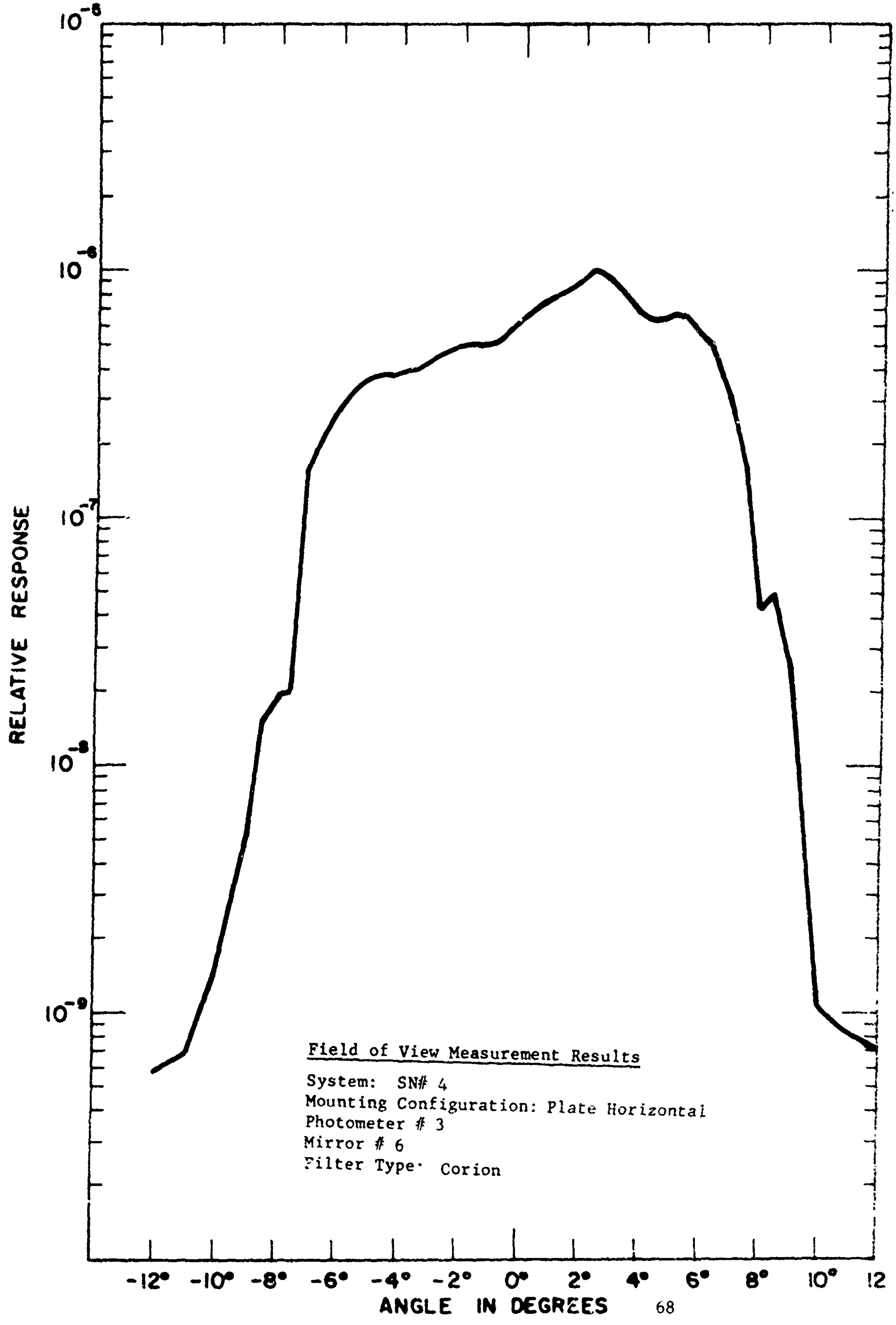

10^{-5}
10^{-6}
10^{-7}
10^{-8}
10^{-9}
RELATIVE RESPONSE
Field of View Measurement Results
System: SN# 4
Mounting Configuration: Plate Horizontal
Photometer # 3
Mirror # 6
Filter Type· Corion
-12° -10° -8° -6° -4° -2° 0° 2° 4° 6° 8° 10° 12
ANGLE IN DEGREES

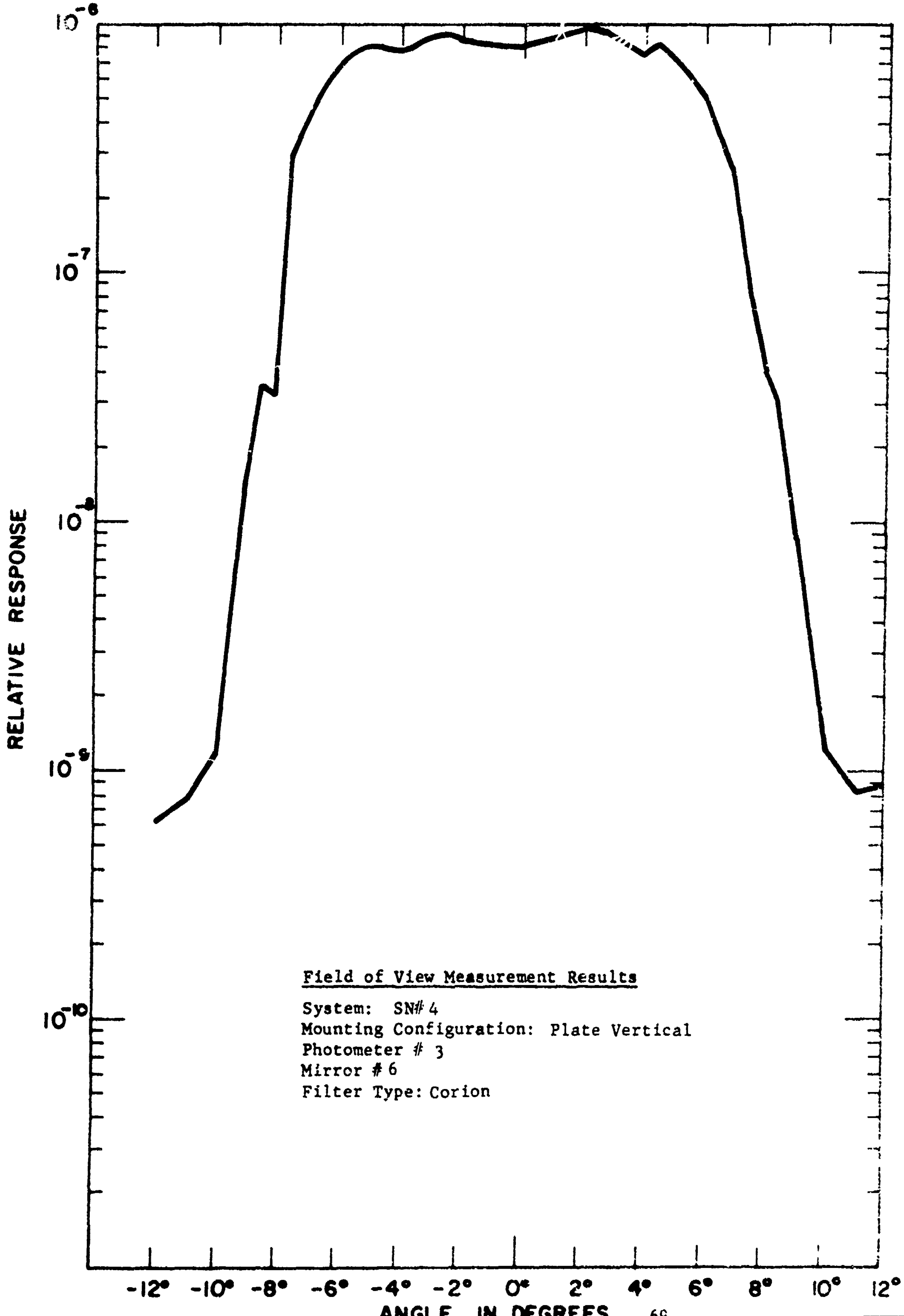
10^{-6}
10^{-7}
10^{-8}
10^{-9}
10^{-10}
RELATIVE RESPONSE
-12° -10° -8° -6° -4° -2° 0° 2° 4° 6° 8° 10° 12°
ANGLE IN DEGREES
Field of View Measurement Results
System: SN# 4
Mounting Configuration: Plate Vertical
Photometer # 3
Mirror # 6
Filter Type: Corion

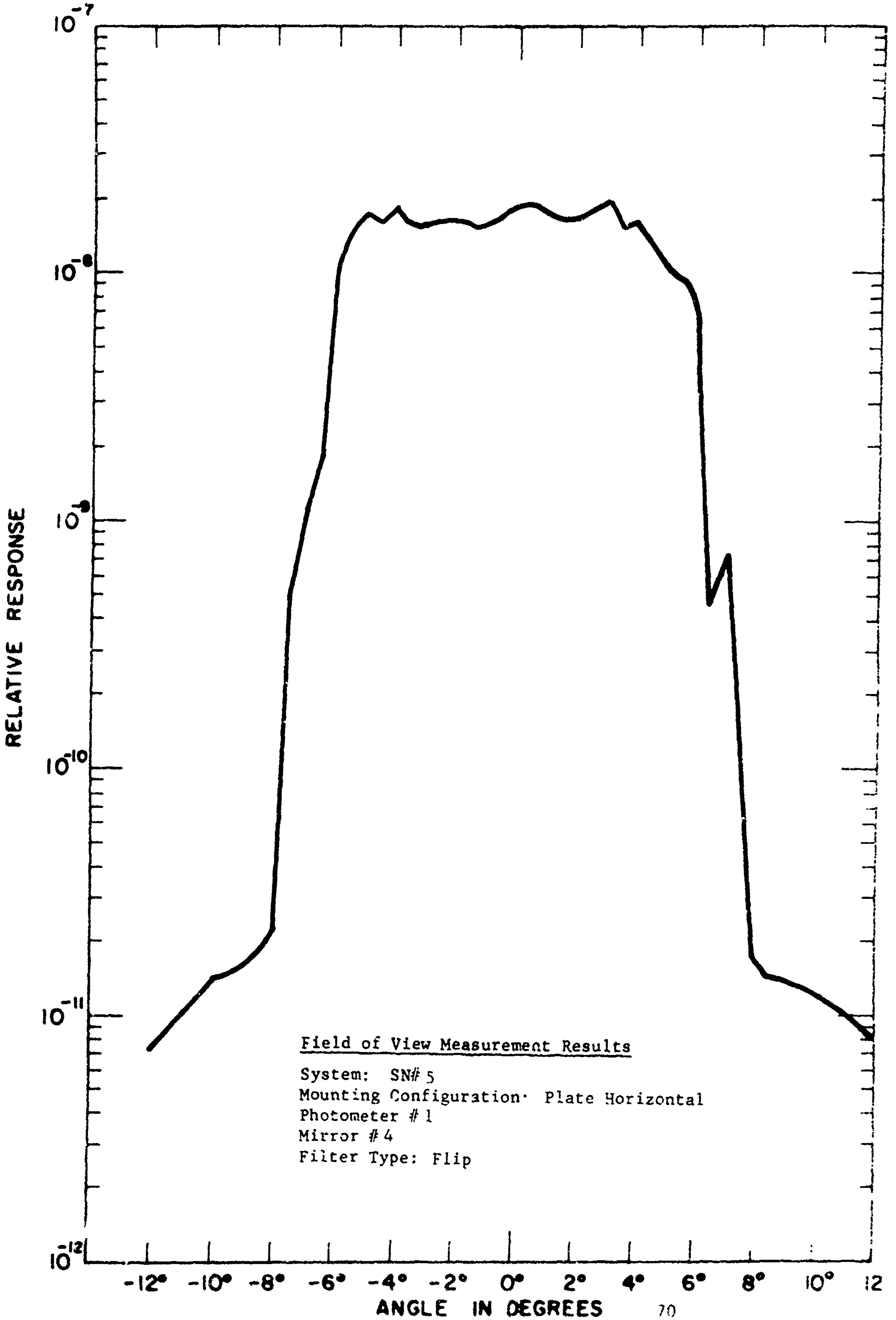
10-7
10-8
10-9
10-10
10-11
10-12
RELATIVE RESPONSE
-12° -10° -8° -6° -4° -2° 0° 2° 4° 6° 8° 10° 12
ANGLE IN DEGREES
Field of View Measurement Results
System: SN# 5
Mounting Configuration: Plate Horizontal
Photometer # 1
Mirror # 4
Filter Type: Flip

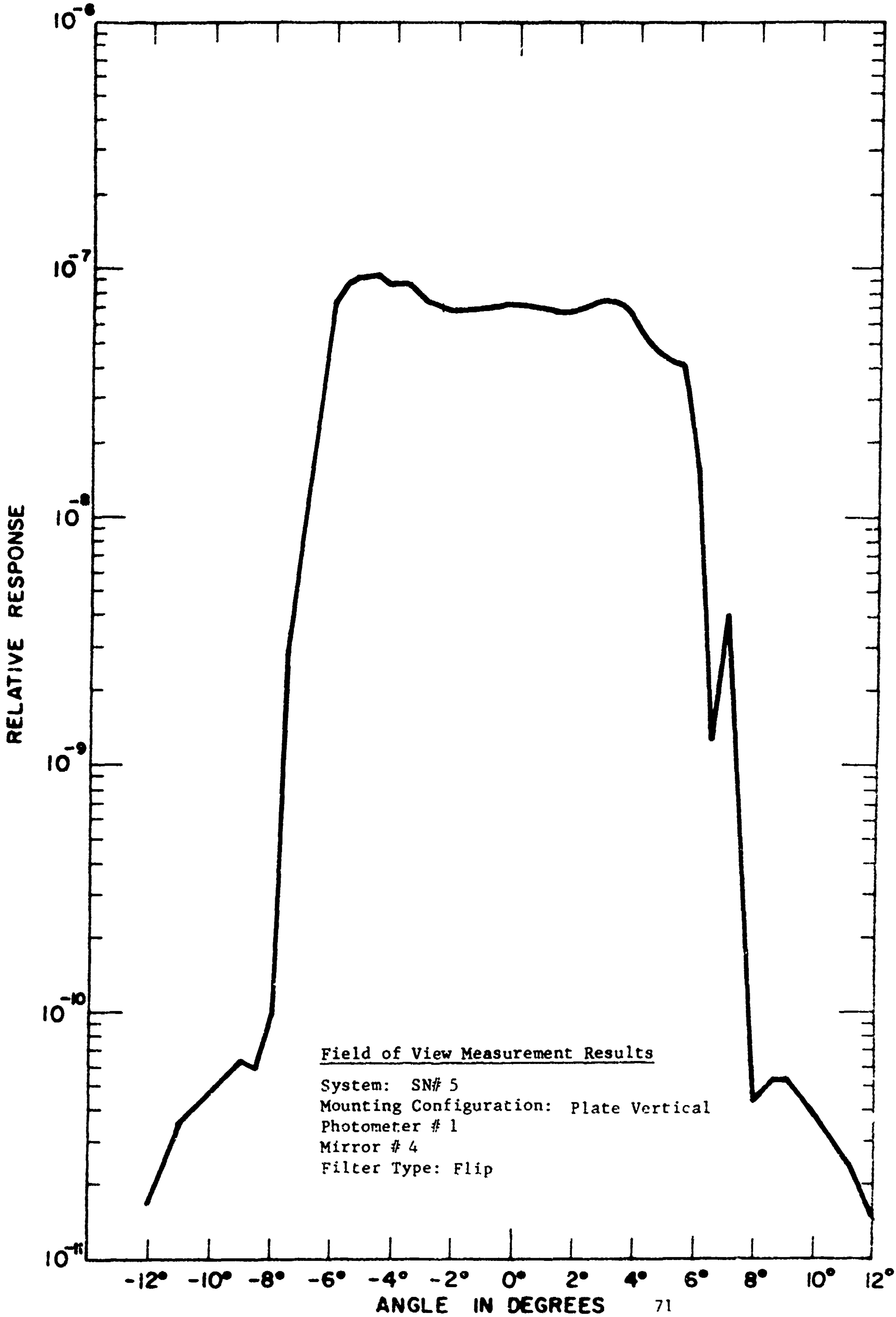

10^{-6}
10^{-7}
10^{-8}
10^{-9}
10^{-10}
10^{-11}
RELATIVE RESPONSE
-12° -10° -8° -6° -4° -2° 0° 2° 4° 6° 8° 10° 12°
ANGLE IN DEGREES
Field of View Measurement Results
System: SN# 5
Mounting Configuration: Plate Vertical
Photometer # 1
Mirror # 4
Filter Type: Flip

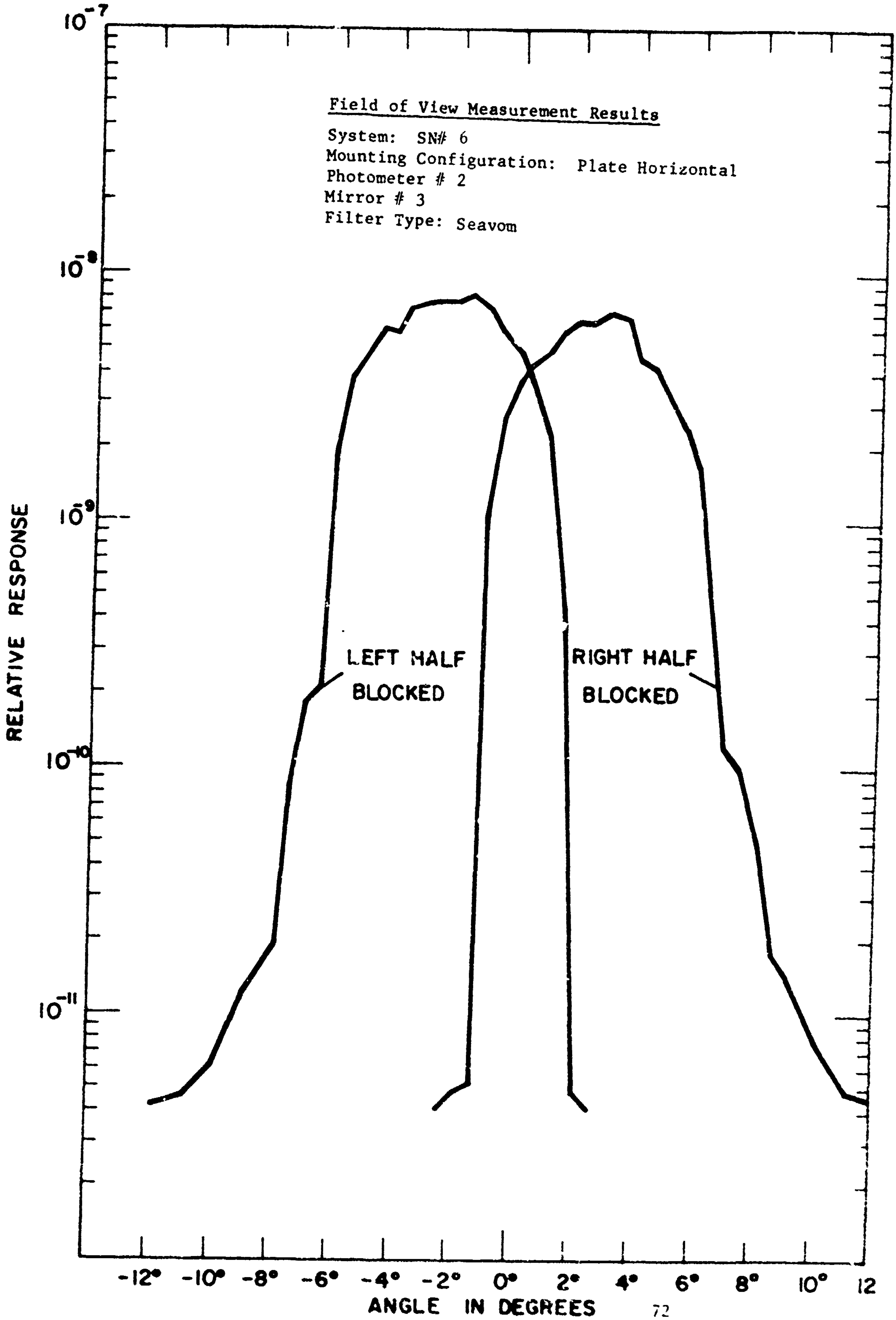
Field of View Measurement Results
System: SN# 6
Mounting Configuration: Plate Horizontal
Photometer # 2
Mirror # 3
Filter Type: Seavom
LEFT HALF BLOCKED
RIGHT HALF BLOCKED
RELATIVE RESPONSE
10^-7
10^-8
10^-9
10^-10
10^-11
-12° -10° -8° -6° -4° -2° 0° 2° 4° 6° 8° 10° 12
ANGLE IN DEGREES

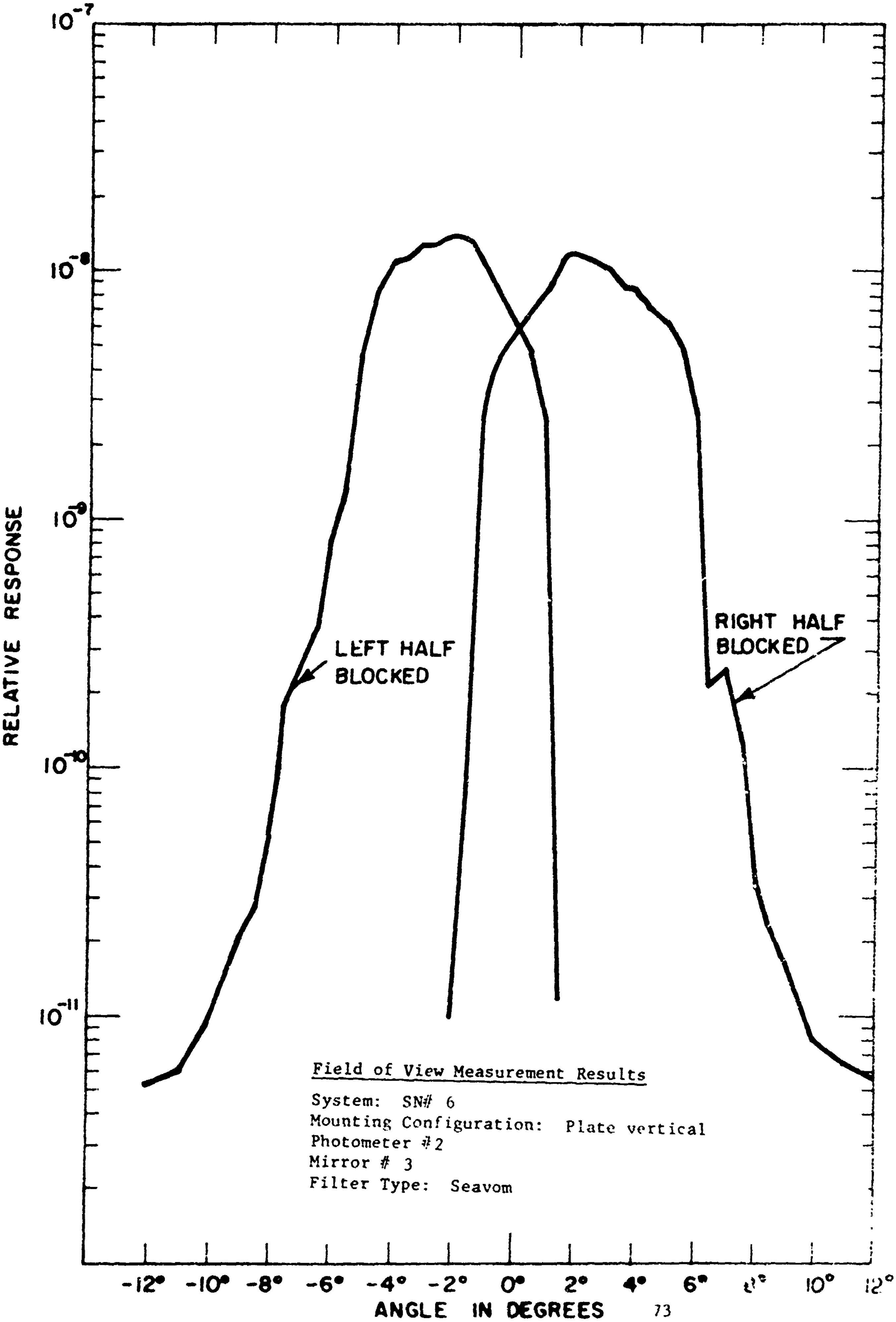

10^{-7}
10^{-8}
10^{-9}
10^{-10}
10^{-11}
RELATIVE RESPONSE
LEFT HALF BLOCKED
RIGHT HALF BLOCKED
Field of View Measurement Results
System: SN# 6
Mounting Configuration: Plate vertical
Photometer #2
Mirror # 3
Filter Type: Seavom
-12° -10° -8° -6° -4° -2° 0° 2° 4° 6° 8° 10° 12°
ANGLE IN DEGREES

APPENDIX B

GCA MODEL DP-2000A KG

A multi-decade logarithmic amplifier is used to measure electron and ion currents. The amplifier is an all electronic solid-state unit which uses no mechanical choppers and no friction contacts and is extremely rugged.

Specifications

Current Range:	10^{-9} to 10^{-5} amps with 10% of a decade accuracy over 10^{-8} to 10^{-5} amps
Output Level: (approximately 1V per decade)	0 to +5 V
Input Power:	10.4V at 10 mA (+12V to +9V) -10.4V at 10 mA (-12V to -9V)
Operating Temperature Range:	$-20^{\circ}C$ to $+70^{\circ}C$
Accuracy: (5 decade range)	Within 1/4 decade over the entire temperature span; within $\pm$ 10% of a decade for a temperature span of 25° to 65° for 10^{-8} to 10^{-5} amps
Size:	1.5" diameter by 0.85" high
Shock:	50,000 g's

APPENDIX C
SUBCARRIER OSCILLATOR
GCA MODEL SC-3100

Subcarrier oscillators of the SC-3100 series are small in size, and ruggedized to meet high accelerations. The subcarrier oscillators are compatible with the standard IRIG telemetry bands and are available for each of the standard eighteen IRIG telemetry channels.

Specifications

Frequencies:	All eighteen IRIG frequencies available
Frequency Deviation:	$\pm$ 7 - 1/2%
Input Impedance:	1MΩ minimum
Output Voltage:	1V peak to peak across 5,000Ω
Output Waveform:	Sine wave at less than 1% distortion
Output Impedance:	1 kΩ maximum
Linearity:	1% of design bandwidth at best straight line
Input Voltage:	0 to +5 VDC
Stability:	The total effects of supply voltage change, temperature, and shock causes the center frequency to change less than 1% of design bandwidth.
Power:	+20 VDC at 3 mA (down to +16V)
Size:	1.5" diameter by 0.3" high

APPENDIX D

SPECIAL PARTS

The following special parts have been incorporated into each photometer.

1. Reticle motor, Globe #18A107
2. Torque motor, Aeroflex #T018W-23P
3. Reticle magnetic sensor, Electro Products #3080
4. Cal lamp, Xenon Corporation #S-300
5. Reed Coil, James Electronics #7809
6. Reed Relay, Hamlin #MRO-2-206
7. Optically coupled isolator, #TIXL109
8. Log Amplifier, GCA Model DP-2000-A-K
9. Linear Amplifier, GCA Model DP-2200-K
10. VCO, GCA Model SC-3100
11. Low Voltage Transformer T1, GCA 107381
12. Low Voltage Transformer T2, GCA 107382
13. High Voltage Transformer T101, GCA 107383
14. High Voltage Transformer T201, GCA 107384
15. High Voltage Transformer T301, GCA 107385
16. Reticle bearing, Kaydon, KAA10AG
17. Reticle drive belt, Kinelogic, 11.437 x .125 x .001, Class IV
18. Reticle motor, Globe, 18A107
19. Flip filter switch, Microswitch, 11S x 21-T
20. Flip filter switch actuator, Microswitch, TX-20
21. Flip filter motor, Aeroflex, TQ18W-23P
22. Flip filter motor bearing, NHBB, SFR166FPEE
23. HV connector "O" ring, Greene, 2-10
24. HV box nipple, Cajon, 1-CN
25. HV box nipple cap, Cajon, 1-CP